Beauty photoproduction at HERA: k_T-factorization versus experimental data

A.V. Lipatov, N.P. Zotov

January 28, 2006

D.V. Skobeltsyn Institute of Nuclear Physics,
M.V. Lomonosov Moscow State University,
119992 Moscow, Russia

Abstract

We present calculations of the beauty photoproduction at HERA collider in the framework of the k_T-factorization approach. Both direct and resolved photon contributions are taken into account. The unintegrated gluon densities in a proton and in a photon are obtained from the full CCFM, from unified BFKL-DGLAP evolution equations as well as from the Kimber-Martin-Ryskin prescription. We investigate different production rates (both inclusive and associated with hadronic jets) and compare our theoretical predictions with the recent experimental data taken by the H1 and ZEUS collaborations. Special attention is put on the $x_\gamma^{\rm obs}$ variable which is sensitive to the relative contributions to the beauty production cross section.

1 Introduction

The beauty production at high energies is a subject of intensive study from both theoretical and experimental points of view. First measurements [1] of the b-quark cross sections at HERA were significantly higher than QCD predictions calculated at next-to-leading order (NLO). Similar observations were made in hadron-hadron collisions at Tevatron [2] and also in photon-photon interactions at LEP2 [3]. In last case, the theoretical NLO QCD predictions are more than three standard deviations below the experimental data. At Tevatron, recent analisys indicates that the overall description of the data can be improved [4] by adopting the non-perturbative fragmentation function of the b-quark into the B-meson: an appropriate treatment of the b-quark fragmentation properties considerably reduces the

disagreement between measured beauty cross section and the corresponding NLO QCD calculations. Recently H1 and ZEUS collaborations have reported important data [5–7] on the beauty photoproduction (both inclusive and associated with hadronic jets) in electron-proton collisions at HERA which refer to small values of the Bjorken scaling variable x. These data are in a reasonable agreement with NLO QCD predictions or somewhat higher. Some disagreement is observed [7] mainly at small decay muon and/or associated jet transverse momenta. But the large excess of the first measurements over NLO QCD, reported [1] by the H1 collaboration, is not confirmed. In the present paper to analyze the H1 and ZEUS data we will apply the so-called k_T-factorization [8, 9] (or semi-hard [10, 11]) approach of QCD since the beauty production at HERA is dominated by the photon-gluon or gluon-gluon fusion (direct and resolved photon contributions, respectively) and therefore sensitive to the gluon densities in a proton and in a photon at small values of x.

The k_T-factorization approach is based on the Balitsky-Fadin-Kuraev-Lipatov (BFKL) [12] or Ciafaloni-Catani-Fiorani-Marchesini (CCFM) [13] gluon evolution which are valid at small x since here large logarithmic terms proportional to $\ln 1/x$ are summed up to all orders of perturbation theory (in the leading logarithmic approximation). It is in contrast with the popular Dokshitzer-Gribov-Lipatov-Altarelli-Parizi (DGLAP) [14] strategy where only large logarithmic terms proportional to $\ln \mu^2$ are taken into account. The basic dynamical quantity of the k_T-factorization approach is the so-called unintegrated ($\mathbf{k}_T$-dependent) gluon distribution $\mathcal{A}(x, \mathbf{k}_T^2, \mu^2)$ which determines the probability to find a gluon carrying the longitudinal momentum fraction x and the transverse momentum $\mathbf{k}_T$ at the probing scale μ^2. The unintegrated gluon distribution can be obtained from the analytical or numerical solution of the BFKL or CCFM evolution equations. Similar to DGLAP, to calculate the cross sections of any physical process the unintegrated gluon density $\mathcal{A}(x, \mathbf{k}_T^2, \mu^2)$ has to be convoluted [8–11] with the relevant partonic cross section $\hat{\sigma}$. But as the virtualities of the propagating gluons are no longer ordered, the partonic cross section has to be taken off mass shell ($\mathbf{k}_T$-dependent). It is in clear contrast with the DGLAP scheme (so-called collinear factorization). Since gluons in initial state are not on-shell and are characterized by virtual masses (proportional to their transverse momentum), it also assumes a modification of their polarization density matrix [10, 11]. In particular, the polarization vector of a gluon is no longer purely transversal, but acquires an admixture of longitudinal and time-like components. Other important properties of the k_T-factorization formalism are the additional contribution to the cross sections due to the integration over the $\mathbf{k}_T^2$ region above μ^2 and the broadening of the transverse momentum distributions due to extra transverse momentum of the colliding partons.

Some applications of the k_T-factorization approach supplemented with the BFKL and CCFM evolution to the b-quark production at high energies were discussed in [15–26]. It was shown [17–21] that the beauty cross section at Tevatron can be consistently described in the framework of this approach. However, a substantial discrepancy between theory and experiment is still found [22–25] for the b-quark production in $\gamma\gamma$ collisions at LEP2, not being cured by the k_T-factorization[1]. At HERA, the inclusive beauty photoproduction has been investigated [18, 22, 26] and comparisons with the first H1 measurements [1] have been done. It was concluded that the k_T-factorization approach provide a reasonable description

[1]Some discussions of this problem may be found in [22, 24].

of the data within the large theoretical and experimental uncertainties. In [18, 26] the Monte-Carlo generator CASCADE [27] has been used to predict the cross section of the b-quark and dijet associated photoproduction. However, all calculations [18, 22, 26] deal with the total cross sections only. A number of important differential cross sections (such as transverse momentum and pseudo-rapidity distributions) has not been considered and comparisons with the recent H1 and ZEUS measurements [5–7] have not been made.

In the present paper we will study the beauty production at HERA in more detail. We investigate a number of different photoproduction rates (in particular, the transverse momentum and pseudo-rapidity distributions of muons which originate from the semi-leptonic decays of b-quarks) and make comparisons with the recent H1 and ZEUS data [5–7]. Both direct ($\gamma g \to b\bar{b}$) and resolved photon contributions ($gg \to b\bar{b}$) will be taken into account[2]. Our analysis covers also both inclusive and dijet associated b-quark production. In last case special attention will be put on the $x_\gamma^{\rm obs}$ variable since this quantity is sensitive to the relative contributions to the cross section from different production mechanisms. One of the purposes of this paper is to investigate the specific k_T-factorization effects in the b-quark production at HERA. In the numerical analysis we test the unintegrated gluon distributions which are obtained from the full CCFM, unified BFKL-DGLAP [31] evolution equations and from the conventional parton densities (using the Kimber-Martin-Ryskin prescription [32]). We would like to note that this study is the continuation of our previous investigations [24, 30] where we have discussed, in particular, the charm production at LEP2 [24] and HERA [30].

The outline of our paper is following. In Section 2 we recall the basic formulas of the k_T-factorization approach with a brief review of calculation steps. In Section 3 we present the numerical results of our calculations and a dicussion. Finally, in Section 4, we give some conclusions.

2 Basic formulas

2.1 Kinematics

We start from the gluon-gluon fusion subprocess. Let p_e and p_p be the four-momenta of the initial electron and proton, k_1 and k_2 the four-momenta of the incoming off-shell gluons, and p_b and $p_{\bar{b}}$ the four-momenta of the produced beauty quarks. In our analysis below we will use the Sudakov decomposition, which has the following form:

$$\begin{aligned} p_b = \alpha_1 p_e + \beta_1 p_p + p_{b\,T}, \quad p_{\bar{b}} = \alpha_2 p_e + \beta_2 p_p + p_{\bar{b}\,T}, \\ k_1 = x_1 p_e + k_{1T}, \quad k_2 = x_2 p_p + k_{2T}, \end{aligned} \tag{1}$$

where k_{1T}, k_{2T}, $p_{b\,T}$ and $p_{\bar{b}\,T}$ are the transverse four-momenta of the corresponding particles. It is important that $\mathbf{k}_{1T}^2 = -k_{1T}^2 \neq 0$ and $\mathbf{k}_{2T}^2 = -k_{2T}^2 \neq 0$. If we make replacement $k_1 \to p_e$ and set $x_1 = 1$ and $k_{1T} = 0$, then we easily obtain more simpler formulas corresponding to photon-gluon fusion subprocess. In the ep center-of-mass frame we can write

$$p_e = \sqrt{s}/2(1,0,0,1), \quad p_p = \sqrt{s}/2(1,0,0,-1), \tag{2}$$

[2] The b-quark excitation processes $bg \to bg$ are automatically included in the k_T-factorization approach, as it was demonstrated in [28–30].

where $s = (p_e + p_p)^2$ is the total energy of the process under consideration and we neglect the masses of the incoming particles. The Sudakov variables are expressed as follows:

$$\begin{aligned} \alpha_1 &= \frac{m_{b\,T}}{\sqrt{s}} \exp(y_b), \quad \alpha_2 = \frac{m_{\bar{b}\,T}}{\sqrt{s}} \exp(y_{\bar{b}}), \\ \beta_1 &= \frac{m_{b\,T}}{\sqrt{s}} \exp(-y_b), \quad \beta_2 = \frac{m_{\bar{b}\,T}}{\sqrt{s}} \exp(-y_{\bar{b}}), \end{aligned} \tag{3}$$

where $m_{b\,T}$ and $m_{\bar{b}\,T}$ are the transverse masses of the produced quarks, and y_b and $y_{\bar{b}}$ are their rapidities (in the ep center-of-mass frame). From the conservation laws we can easily obtain the following conditions:

$$x_1 = \alpha_1 + \alpha_2, \quad x_2 = \beta_1 + \beta_2, \quad \mathbf{k}_{1T} + \mathbf{k}_{2T} = \mathbf{p}_{b\,T} + \mathbf{p}_{\bar{b}\,T}. \tag{4}$$

The variable $x_\gamma^{\rm obs}$ is often used in the analysis of the data which contain the dijet samples. This variable, which is the fraction of the photon momentum contributing to the production of two hadronic jets with transverse energies $E_T^{\rm jet_1}$ and $E_T^{\rm jet_2}$, experimentally is defined [6, 7] as

$$x_\gamma^{\rm obs} = \frac{E_T^{\rm jet_1} e^{-\eta^{\rm jet_1}} + E_T^{\rm jet_2} e^{-\eta^{\rm jet_2}}}{2yE_e}, \tag{5}$$

where yE_e is the initial photon energy and $\eta^{\rm jet_i}$ are the pseudo-rapidities of these jets. The pseudo-rapidities $\eta^{\rm jet_i}$ are defined as $\eta^{\rm jet_i} = -\ln\tan(\theta^{\rm jet_i}/2)$, where $\theta^{\rm jet_i}$ are the polar angles of the jets with respect to the proton beam. Note that the selection of $x_\gamma^{\rm obs} > 0.75$ and $x_\gamma^{\rm obs} < 0.75$ yields samples enriched in direct and resolved photon processes, respectively.

2.2 Cross section for beauty photoproduction

The main formulas for the total and differential beauty production cross sections were obtained in our previous papers [19, 24]. Here we recall some of them. In general case, the cross section σ according to k_T-factorization theorem can be written as a convolution

$$\sigma = \sigma_0 \int \frac{dz}{z}\, d\mathbf{k}_T^2\, C(x/z, \mathbf{k}_T^2, \mu^2) \mathcal{A}(x, \mathbf{k}_T^2, \mu^2), \tag{6}$$

where $C(x, \mathbf{k}_T^2, \mu^2)$ is the coefficient function corresponding to relevant partonic subprocess under consideration. So, the direct photon contribution to the differential cross section of $\gamma p \to b\bar{b} + X$ process is given by

$$\frac{d\sigma^{\rm (dir)}(\gamma p \to b\bar{b} + X)}{dy_b\, d\mathbf{p}_{b\,T}^2} = \int \frac{|\bar{\mathcal{M}}|^2(\gamma g^* \to b\bar{b})}{16\pi (x_2 s)^2 (1-\alpha_1)} \mathcal{A}(x_2, \mathbf{k}_{2T}^2, \mu^2) d\mathbf{k}_{2T}^2 \frac{d\phi_2}{2\pi} \frac{d\phi_b}{2\pi}, \tag{7}$$

where $|\bar{\mathcal{M}}|^2(\gamma g^* \to b\bar{b})$ is the squared off-shell matrix element which depends on the transverse momentum $\mathbf{k}_{2T}^2$, ϕ_2 and ϕ_b are the azimuthal angles of the initial virtual gluon and the produced quark, respectively. The formula for the resolved photon contribution can be obtained by the similar way. But one should keep in mind that convolution in (6) should

be made also with the unintegrated gluon distribution $\mathcal{A}_\gamma(x, \mathbf{k}_T^2, \mu^2)$ in a photon. The final expression for the differential cross section has the form

$$\frac{d\sigma^{(\rm res)}(\gamma p \to b\bar{b} + X)}{dy_b\, d\mathbf{p}_{b\,T}^2} = \int \frac{|\bar{\mathcal{M}}|^2(g^* g^* \to b\bar{b})}{16\pi (x_1 x_2 s)^2} \times$$
$$\times \mathcal{A}_\gamma(x_1, \mathbf{k}_{1T}^2, \mu^2) \mathcal{A}(x_2, \mathbf{k}_{2T}^2, \mu^2) d\mathbf{k}_{1T}^2 d\mathbf{k}_{2T}^2 dy_{\bar{b}} \frac{d\phi_1}{2\pi} \frac{d\phi_2}{2\pi} \frac{d\phi_b}{2\pi}, \tag{8}$$

where ϕ_1 is the azimuthal angle of the initial virtual gluon having fraction x_1 of a initial photon longitudinal momentum. It is important that squared off-shell matrix element $|\bar{\mathcal{M}}|^2(g^* g^* \to b\bar{b})$ depends on the both transverse momenta $\mathbf{k}_{1T}^2$ and $\mathbf{k}_{2T}^2$. The analytic expressions for the $|\bar{\mathcal{M}}|^2(\gamma g^* \to b\bar{b})$ and $|\bar{\mathcal{M}}|^2(g^* g^* \to b\bar{b})$ have been evaluated in our previous papers [19, 24]. Note that if we average (7) and (8) over $\mathbf{k}_{1T}$ and $\mathbf{k}_{2T}$ and take the limit $\mathbf{k}_{1T}^2 \to 0$ and $\mathbf{k}_{2T}^2 \to 0$, then we obtain well-known formulas corresponding to the leading-order (LO) QCD calculations.

The recent experimental data [5–7] taken by the H1 and ZEUS collaborations refer to the b-quark photoproduction in ep collisions, where electron is scattered at small angle and the mediating photon is almost real ($Q^2 \sim 0$). Therefore γp cross sections (7) and (8) needs to be weighted with the photon flux in the electron:

$$d\sigma(ep \to b\bar{b} + X) = \int f_{\gamma/e}(y) dy\, d\sigma(\gamma p \to b\bar{b} + X), \tag{9}$$

where y is a fraction of the initial electron energy taken by the photon in the laboratory frame, and we use the Weizacker-Williams approximation for the bremsstrahlung photon distribution from an electron:

$$f_{\gamma/e}(y) = \frac{\alpha_{em}}{2\pi} \left(\frac{1 + (1-y)^2}{y} \ln \frac{Q^2_{\rm max}}{Q^2_{\rm min}} + 2m_e^2 y \left(\frac{1}{Q^2_{\rm max}} - \frac{1}{Q^2_{\rm min}} \right) \right). \tag{10}$$

Here α_{em} is Sommerfeld's fine structure constant, m_e is the electron mass, $Q^2_{\rm min} = m_e^2 y^2/(1-y)^2$ and $Q^2_{\rm max} = 1\,{\rm GeV}^2$, which is a typical value for the recent photoproduction measurements at HERA.

The multidimensional integration in (7), (8) and (9) has been performed by means of the Monte Carlo technique, using the routine VEGAS [33]. The full C++ code is available from the authors on request[3]. This code is practically identical to that used in [30], with exception that now we apply it to calculate beauty production instead charm.

3 Numerical results

We now are in a position to present our numerical results. First we describe our theoretical input and the kinematical conditions.

[3] lipatov@theory.sinp.msu.ru

3.1 Theoretical uncertainties

There are several parameters which determined the normalization factor of the cross sections (7) and (8): the beauty mass m_b, the factorization and normalisation scales μ_F and μ_R and the unintegrated gluon distributions in a proton $\mathcal{A}(x, \mathbf{k}_T^2, \mu^2)$ and in a photon $\mathcal{A}_\gamma(x, \mathbf{k}_T^2, \mu^2)$.

Concerning the unintegrated gluon densities in a proton, in the numerical calculations we used five different sets of them, namely the J2003 (set 1 — 3) [21], KMS [31] and KMR [32]. All these distributions are widely discussed in the literature (see, for example, review [34, 35] for more information). Here we only shortly discuss their characteristic properties. First, three sets of the J2003 gluon density have been obtained [21] from the numerical solution of the full CCFM equation. The input parameters were fitted to describe the proton structure function $F_2(x, Q^2)$. Note that the J2003 set 1 and J2003 set 3 densities contain only singular terms in the CCFM splitting function $P_{gg}(z)$. The J2003 set 2 gluon density takes into account the additional non-singlular terms[4]. These distributions have been applied in the analysis of the forward jet production at HERA and charm and bottom production at Tevatron [21] (in the framework of Monte-Carlo generator CASCADE) and have been used also in our calculations [30].

Another set (the KMS) [31] was obtained from a unified BFKL-DGLAP description of $F_2(x, Q^2)$ data and includes the so-called consistency constraint [36]. The consistency constraint introduces a large correction to the LO BFKL equation. It was argued [37] that about 70% of the full NLO corrections to the BFKL exponent Δ are effectively included in this constraint. The KMS gluon density is successful in description of the beauty production at Tevatron [17, 19] and J/ψ meson photo- and leptoproduction at HERA [38, 39].

The last, fifth unintegrated gluon distribution $\mathcal{A}(x, \mathbf{k}_T^2, \mu^2)$ used here (the so-called KMR distribution) is the one which was originally proposed in [32]. The KMR approach is the formalism to construct unintegrated gluon distribution from the known conventional parton (quark and gluon) densities. It accounts for the angular-ordering (which comes from the coherence effects in gluon emission) as well as the main part of the collinear higher-order QCD corrections. The key observation here is that the μ dependence of the unintegrated parton distribution enters at the last step of the evolution, and therefore single scale evolution equations (DGLAP or unified BFKL-DGLAP) can be used up to this step. Also it was shown [32] that the unintegrated distributions obtained via unified BFKL-DGLAP evolution are rather similar to those based on the pure DGLAP equations. It is because the imposition of the angular ordering constraint is more important [32] than including the BFKL effects. Based on this point, in our further calculations we use much more simpler DGLAP equation up to the last evolution step[5]. Note that the KMR parton densities in a proton were used, in particular, to describe the prompt photon photo- and hadroproduction at HERA [41] and Tevatron [42, 43].

In the case of a real photon, we have tested two different sets of the unintegrated gluon densities $\mathcal{A}_\gamma(x, \mathbf{k}_T^2, \mu^2)$. First of them was obtained [23] from the numerical solution of the full CCFM equation (which has been also formulated for the photon). Here we will use this gluon density together with the three sets of the J2003 distribution when calculating the

[4] See Ref. [21] for more details.

[5] We have used the standard GRV (LO) parametrizations [40] of the collinear quark and gluon densities.

resolved photon contribution (8). Also in order to obtain the unintegrated gluon density in a photon we will apply the KMR method to the standard GRV parton distributions [40]. In the numerical calculations we will use it together with the KMR distributions in a proton. Note that both gluon densities $\mathcal{A}_\gamma(x, \mathbf{k}_T^2, \mu^2)$ discussed here have been already applied in the analysis of the heavy (charm and beauty) quark [22–25] and J/ψ meson [24, 25] production in $\gamma\gamma$ collisions at LEP2.

We would like to point out that at present there is not the unintegrated gluon distribution corresponding to the unified BFKL-DGLAP evolution in a photon. Therefore we will not take into account the resolved photon contribution (8) in the case of KMS gluon.

Also the significant theoretical uncertainties in our results connect with the choice of the factorization and renormalization scales. First of them is related to the evolution of the gluon distributions, the other is responsible for the strong coupling constant $\alpha_s(\mu_R^2)$. The optimal values of these scales are such that the contribution of higher orders in the perturbative expansion is minimal. As it often done [11, 15–26, 44] for beauty production, we choose the renormalization and factorization scales to be equal: $\mu_R = \mu_F = \mu = \sqrt{m_b^2 + \langle \mathbf{p}_T^2 \rangle}$, where $\langle \mathbf{p}_T^2 \rangle$ is set to the average $\mathbf{p}_T^2$ of the beauty quark and antiquark[6]. Note that in the present paper we concentrate mostly on the non-collinear gluon evolution in the proton and do not study the scale dependence of our results. To completeness, we take the b-quark mass $m_b = 4.75$ GeV and use LO formula for the coupling constant $\alpha_s(\mu^2)$ with $n_f = 4$ active quark flavours at $\Lambda_{\rm QCD} = 200$ MeV, such that $\alpha_s(M_Z^2) = 0.1232$.

3.2 Inclusive beauty photoproduction

The recent experimental data [5–7] for the inclusive beauty photoproduction at HERA comes from both the H1 and ZEUS collaborations. The b-quark total cross section for $p_T > p_T^{\rm min}$ as well as the beauty transverse momentum distribution have been determined. The ZEUS data [5, 6] refer to the kinematical region[7] defined by $|\eta^b| < 2$ and $Q^2 < 1$ GeV^2, where η^b is the beauty pseudo-rapidity. The fraction y of the electron energy transferred to the photon is restricted to the range $0.2 < y < 0.8$.

In Figs. 1 and 2 we show our predictions in comparison to the ZEUS data [5, 6]. The solid, dashed, dash-dotted, dotted and short dash-dotted curves correspond to the results obtained with the J2003 set 1 — 3, KMR and KMS unintegrated gluon densities, respectively. One can see that overall agreement between our predictions and experimental data is a very good. All three sets of the J2003 distribution as well as the KMS gluon density give results which are rather close to each other (except large p_T^b region where the KMS density predicts more hard behaviour). We find also a some enhancement of the estimated cross sections as compared with the collinear NLO QCD calculations which lie somewhat below the measurements but still agree with the data within the scale uncertainties. This enhancement comes, in particular, from the non-zero transverse momentum of the incoming off-shell gluons. Note that the KMR gluon distribution gives results which lie below the ZEUS data and which are very similar to the NLO QCD predictions. This observation coincides with

[6] We use special choice $\mu^2 = \mathbf{k}_T^2$ in the case of KMS gluon, as it was originally proposed in [31].

[7] Here and in the following all kinematic quantities are given in the laboratory frame where positive OZ axis direction is given by the proton beam.

Source	$\sigma(ep \to e'bb + X)$ [nb]
H1 measurement [1]	14.8 ± 1.3 (stat.) $^{+3.3}_{-2.8}$ (sys.)
CASCADE [26]	$5.2^{+1.1}_{-0.9}$
J2003 set 1	6.78
J2003 set 2	6.62
J2003 set 3	7.16
KMR	3.91
KMS	7.57

Table 1: The total cross section of the inclusive beauty photoproduction in electron-proton collisions at $Q^2 < 1$ GeV^2.

the ones [41]. Such underestimation can be explained by the fact that leading logarithmic terms proprtional to $\ln 1/x$ are not included into the KMR formalism.

Also the total inclusive beauty cross section $\sigma(ep \to eb\bar{b} + X)$ has been measured [1] by the H1 collaboration and it was found to be equal to 14.8 ± 1.3 (stat.) $^{+3.3}_{-2.8}$ (sys.) nb for $Q^2 < 1$ GeV^2. The collinear NLO QCD calculations predict a cross section which is about a factor of 4 below the H1 measurements [1]. The results of our calculations supplemented with the different unintegrated gluon densities are collected in Table 1. Also the predictions of the Monte-Carlo generator CASCADE [26] are shown for comparison. One can see that earlier H1 data [1] exceed our theoretical estimations by a factor about 2. However, recent analysis which has been performed in [6, 7] does not confirm the results of the first measurements [1]. So, the cross section for muon coming from b decays in dijet photoproduction events was found [7] to be significantly lower than one reported in [1]. Therefore we can expect that the inclusive b-quark cross section (which can be obtained after extrapolation of dijet and muon cross section to the full phase space) will be reduced and agreement with our predictions will be significantly improved.

In general, we can conclude that the cross sections of inclusive beauty photoproduction calculated in the k_T-factorization formalism (supplemented with the CCFM or unified BFKL-DGLAP evolution) are larger by $30 - 40\%$ than ones calculated at NLO level of collinear QCD. Our results for the total and differential cross sections are in a better agreement with the H1 and ZEUS data than the NLO QCD predictions. We find also that the individual contributions from the photon-gluon and gluon-gluon fusion to the inclusive b-quark cross section in the k_T-factorization approach is about 85 and 15%, respectively. This is in agreement with the results presented in [22] where the KMR and GBW unintegrated gluon densities has been used.

3.3 Dijet associated beauty photoproduction

Now we demonstrate how the k_T-factorization approach can be used to calculate the semi-inclusive beauty photoproduction rates. The basic photon-gluon or gluon-gluon fusion subprocesses give rise to two high-energy b-quarks, which can further evolve into hadron jets. In our calculations the produced quarks (with their known kinematical parameters) were taken to play the role of the final jets. These two quarks are accompanied by a number

of gluons radiated in the course of the gluon evolution. As it has been noted in [28], on the average the gluon transverse momentum decreases from the hard interaction block towards the proton. We assume that the gluon emitted in the last evolution step and having the four-momenta k' compensates the whole transverse momentum of the gluon participating in the hard subprocess, i.e. $\mathbf{k'}_T \simeq -\mathbf{k}_T$. All the other emitted gluons are collected together in the proton remnant, which is assumed[8] to carry only a negligible transverse momentum compared to $\mathbf{k'}_T$. This gluon gives rise to a final hadron jet with $E_T^{\rm jet} = |\mathbf{k'}_T|$ in addition to the jet produced in the hard subprocess. From these three hadron jets we choose the two ones carrying the largest transverse energies, and then compute the beauty and associated dijet photoproduction rates.

The recent experimental data [6, 7] on the beauty and associated dijet production at HERA come from both H1 and ZEUS collaborations. The ZEUS data [6] refer to the kinematical region defined by $0.2 < y < 0.8$, $Q^2 < 1$ GeV^2 and given for jets with $p_T^{\rm jet_1} > 7$ GeV, $p_T^{\rm jet_2} > 6$ GeV and $|\eta^{\rm jet}| < 2.5$. The measured cross sections have been presented for muons coming from semileptonic b decays in dijet events with $p_T^\mu > 2.5$ GeV and $-1.6 < \eta^\mu < 2.3$. The more recent H1 data [7] refer to the same kinematical region except another muon pseudo-rapidity requirement: $-0.55 < \eta^\mu < 1.1$. To produce muons from b-quarks in our theoretical calculations, we first convert b-quarks into B-hadrons using the Peterson fragmentation function [45] and then simulate their semileptonic decay according to the standard electroweak theory[9]. Our default set of the fragmentation parameter is $\epsilon_b = 0.0035$.

So, the transverse momentum and pseudo-rapidity distributions of the b-quark decay muon for different kinematical region are shown in Figs. 3 — 6 in comparison to the HERA data. One can see that calculated cross sections (using the J2003 and KMS unintegrated gluon densities) agree very well with the experimental data except the low p_T^μ region ($p_T^\mu < 3$ GeV) in Fig. 4. Note, however, that the behaviour of measured cross sections in this region is very different from each other in the H1 and ZEUS data. The p_T^μ distribution measured [7] by the H1 collaboration falls steeply with increasing transverse momentum p_T^μ. The similar situation is observed also for the cross section measured as a function of the transverse momentum of leading jet $p_T^{\rm jet}$ (see Fig. 7). Our calculations give a less steep behaviour and are lower than the H1 data in the lowest momentum bin by a factor of 2.5. But at higher transverse momenta p_T^μ better agreement is obtained. Note that in the case of $p_T^{\rm jet}$ distribution the discrepancy at low $p_T^{\rm jet}$ is smaller, is about 1.5 times only. In contrast, a good description of the ZEUS data [6] (both in normalization and shape) for all values of p_T^μ is observed (see Fig. 3). Therefore there is some inconsistency between the data.

Also the ZEUS collaboration have presented the data on the transverse momentum and pseudo-rapidity distributions of the jets associated with the muon (so-called μ-jet) or B-hadron (b-jet). These jets reproduce the kinematic of the b (or $\bar{b}$) quark in a good approximation. The μ-jet is defined as the jet containing the B-hadron that decays into the muon. Similarly, the b-jet is defined as the jet containing the B (or $\bar{B}$) hadron. In Figs. 8 — 11 we show our predictions for the transverse momentum and pseudo-rapidity distributions of the μ-jet and b-jet in comparison to the ZEUS measurements [6]. One can see that

[8]Note that such assumption is also used in the KMR formalism.

[9]Of course, the muon transverse momenta spectra are sensitive to the fragmentation functions. However, this dependence is expected to be small as compared with the uncertainties coming from the unintegrated gluon densities in a proton and in a photon.

J2003 and KMS gluon densities give results which agree well with the data, although slightly overestimate the data at low $p_T^{\mu-\mathrm{jet}}$ (see Fig. 8).

We would like to note that the KMS gluon provides a more hard transverse momentum distribution of the final muon (or jets) as compared with other unintegrated densities under consideration. Similar effect we have observed in the case of the inclusive beauty photoproduction (in a previous section). Another interesting observation is that the dotted curves which obtained using the KMR unintegrated gluon lie below the H1 and ZEUS data everywhere. This fact confirms the assumption which was made in [41] that the KMR formalism results in some underestimation of the calculated cross sections. Also it is interesting that the difference in normalization between the KMS and J2003 predictions is rather small, is about 20% only. However, it is in the contrast with the D^* and dijet associated photoproduction at HERA which has been investigated in our previous paper [30], where we have found a relative large enhancement of the cross sections calculated using the KMS gluon density. The possible explanation of this fact is that the large b-quark or J/ψ meson mass (which provide a hard scale) make predictions of the perturbation theory of QCD more applicable.

Next we concentrate on the very interesting subject of study which is connected with the individual contributions from the direct and resolved photon mechanisms to the cross section in the k_T-factorization approach. As it was already mentioned above, the x_γ^{obs} variable (which corresponds at leading order to the fraction of the exchanged photon momentum in the hard scattering process) provides a tool to investigate the relative importance of different contributions. In LO approximation, direct photon events at parton level have $x_\gamma^{\mathrm{obs}} \sim 1$, while the resolved photon events populate the low values of x_γ^{obs}. The same situation is observed in a NLO calculations, because in the three parton final state any of these partons are allowed to take any kinematically accessible value. In the k_T-factorization formalism the hardest transverse momentum parton emission can be anywhere in the evolution chain, and does not need to be closest to the photon as required by the strong μ^2 ordering in DGLAP. Thus, if the two hardest jets are produced by the $b\bar{b}$ pair, then x_γ^{obs} is close to unity, but if a gluon from the initial cascade and one of the final b-quarks form the two hardest transverse momentum jets, then $x_\gamma^{\mathrm{obs}} < 1$. This statement is clearly demonstrated in Fig. 12 where separately shown the contributions from the photon-gluon (dashed curve) and gluon-gluon fusion (dash-dotted curve) subprocesses. The solid curve represents the sum of both these contributions. We have used here the KMR unintegrated gluon density for illustration. As it was expected, the gluon-gluon fusion events (with a gluon coming from the photon) are distributed over the whole x_γ^{obs} range. It is clear that these events play important role at small values of x_γ^{obs}. Next, in agreement with the expectation for direct photon processes, the peak at high values of the x_γ^{obs} is observed. However, one can see that off-shell photon-gluon fusion results also in substantial tail at small values of x_γ^{obs}. The existence of this plateau in the collinear approximation of QCD usually is attributted to the heavy quark excitation from resolved photon. In the k_T-factorization approach such plateau indicates the fact that the gluon radiated from evolution cascade appears to be harder than b-quarks (produced in hard parton interaction) in a significant fraction of events [28–30].

In Fig. 13 and 14 we confront the x_γ^{obs} distributions calculated in different kinematical regions with the HERA data [6, 7]. One can see that the J2003 and KMR unintegrated gluon densities give a reasonable description of the data but tend to slightly underestimate them at middle and low x_γ^{obs}. In the case of KMS gluon this discrepancy is more significant

Source	$\sigma(ep \to ebb + X \to ejj\mu + X')$ [pb]
H1 measurement [7]	38.4 ± 3.4 (stat.) ± 5.4 (sys.)
NLO QCD (FMNR) [44]	$23.8^{+7.4}_{-5.1}$
CASCADE (J2003 set 2)	22.6
PYTHIA [46]	20.9
J2003 set 1	28.37
J2003 set 2	27.33
J2003 set 3	29.25
KMR	17.43
KMS	33.87
KMS ($m_b = 4.5$ GeV, $\Lambda_{\rm QCD} = 250$ MeV)	38.84

Table 2: The total cross section of the beauty and associated dijet photoproduction obtained in the kinematic range $-0.55 < \eta^\mu < 1.1$, $p_T^\mu > 2.5$ GeV, $Q^2 < 1$ GeV^2, $0.2 < y < 0.8$, $p_T^{\rm jet_1} > 7$ GeV, $p_T^{\rm jet_2} > 6$ GeV and $|\eta^{\rm jet}| < 2.5$.

since the contribution from the gluon-gluon fusion subprocess are not taken into account here. The Monte-Carlo generator CASCADE [27] (which generates low $x_\gamma^{\rm obs}$ events via initial state gluon radiation without using a gluon density in a photon) also underestimate [7] the cross sections at low $x_\gamma^{\rm obs}$. Note that the shapes of $x_\gamma^{\rm obs}$ distributions predicted by the J2003 and KMR densities differs from each other. This fact is connected with different properties of corresponding unintegrated gluon distributions in a proton and in a photon. In general, from Fig. 12 — 14 we can conclude that the gluon-gluon fusion contribution is important in description of the experimental data and that the behaviour of calculated $x_\gamma^{\rm obs}$ distributions at low values of $x_\gamma^{\rm obs}$ is strongly depends on the unintegrated gluon densities used. However, our calculations still reasonable agree with the H1 and ZEUS data within the theoretical and experimental uncertainties.

Now we turn to the total cross section of b-quark and associated dijet photoproduction. The ZEUS collaboration has presented [6] the results for forward, barrel and rear muon-chambers regions which defined by $-1.6 < \eta^\mu < -0.9$, $p_T^\mu > 2.5$ GeV (rear), $-0.9 < \eta^\mu < 1.3$, $p_T^\mu > 2.5$ GeV (barrel) and $1.48 < \eta^\mu < 2.3$, $p_T^\mu > 2.5$ GeV, $p^\mu > 4$ GeV (forward). In Fig. 15 we display the results of our calculations in comparison to the recent ZEUS data. One can see that our predictions (supplemented with the J2003 and KMS gluon densities) agree well with the measurements in the barrel region but underestimate the data in rear and forward ones. The main discrepancy is found in forward kinematical region where our predictions are below the data by a factor of 1.5. In Table 2 we compare the calculated cross section with the H1 data [7] which has been obtained in another kinematical region (defined above). The predictions of Monte-Carlo programs PYTHIA [46], CASCADE [27] as well as NLO QCD calculations (FMNR) [44] are also shown for comparison. Note that these results are in a good agreement with each other but are about 1.5 standard deviations below [7] the data. Our predictions are somewhat higher but still lie below the data, too. However, this discrepancy is not dramatic, because some reasonable variations in beauty mass m_b, energy scale μ^2 or $\Lambda_{\rm QCD}$ parameter, namely $4.5 < m_b < 5$ GeV, $\mu_0^2/2 < \mu^2 < 2\mu_0^2$ (where μ_0 is the transverse mass of produced b-quark) and $150 < \Lambda_{\rm QCD} < 250$ MeV, can completely eliminate the visible

disagreement. To be precise, we have repeated our calculations using the KMS gluon density with the $m_b = 4.5$ GeV and $\Lambda_{\rm QCD} = 250$ MeV. We obtained the value $\sigma = 38.84$ pb which is close to the experimental data point $\sigma = 38.4 \pm 3.4 \pm 5.4$ pb.

Finally, we would like to note that in according to the analysis [6, 7] which was done by the H1 and ZEUS collaborations, in order to obtain a realistic comparison of the data and NLO QCD calculations the corrections for hadronisation should be taken into account in the predictions. The correction factors are typically $0.8 - 1.1$ depending on a bin [6, 7]. These factors are not accounted for in our analysis.

4 Conclusions

We have investigated the beauty production in electron-proton collisions at HERA in the k_T-factorization QCD approach. The different photoproduction rates (both inclusive and associated with hadronic jets) have been studied. We took into account both the direct and resolved photon contribution. In numerical analysis we have used the unintegrated gluon densities which are obtained from the full CCFM, from unified BFKL-DGLAP evolution equations (KMS) as well as from the Kimber-Martin-Ryskin prescription. Our investigations were based on LO off-mass shell matrix elements for the photon-gluon and gluon-gluon fusion subprocesses. Special attention has been drawn to the $x_\gamma^{\rm obs}$ variable since this quantity is sensitive to relative contributions to the cross section from the different production mechanisms. We demonstrate the importance of gluon-gluon fusion subprocess in description of the experimental data at low values of $x_\gamma^{\rm obs}$.

We have shown that the k_T-factorization approach supplemented with the CCFM or BFKL-DGLAP evolved unintegrated gluon distributions (the J2003 or KMS densities) reproduces well the numerous HERA data on beauty production. At the same time we have obtained that the Kimber-Martin-Ryskin formalism results in some underestimation of the cross sections. This shows the importance of a detail understanding of the non-collinear parton evolution process.

5 Acknowledgements

The authors are very grateful to S.P. Baranov for encouraging interest and very helpful discussions, L.K. Gladilin for reading of the manuscript and very useful remarks. This research was supported in part by the FASI of Russian Federation (grant NS-1685.2003.2).

References

[1] C. Adloff *et al.* (H1 Collaboration), Phys. Lett. B **467**, 156 (1999); Erratum: *ibid* B **518**, 331 (2001).

[2] F. Abe *et al.* (CDF Collaboration), Phys. Rev. D **55**, 2546 (1997);
D. Acosta *et al.* (CDF Collaboration), Phys. Rev. D **65**, 052002 (2002);
S. Abachi *et al.* (D0 Collaboration), Phys. Lett. B **487**, 264 (2000).

[3] M. Acciari *et al.* (L3 Collaboration), Phys. Lett. B **503**, 10 (2001);
P. Achard *et al.* (L3 Collaboration), Phys. Lett. B **619**, 71 (2005);
G. Abbiendi *et al.* (OPAL Collaboration), Eur. Phys. J. C **16**, 579 (2000).

[4] M. Cacciari and P. Nason, Phys. Rev. Lett. **89**, 122003 (2002);
M. Cacciari, S. Frixione, M.L. Mangano, P. Nason, and G. Ridolfi, JHEP **0407**, 033 (2004).

[5] J. Breitweg *et al.* (ZEUS Collaboration), Eur. Phys. J. C **18**, 625 (2001).

[6] S. Chekanov *et al.* (ZEUS Collaboration), Phys. Rev. D **70**, 012008 (2004).

[7] A. Aktas *et al.* (H1 Collaboration), Eur. Phys. J. C **41**, 453 (2005).

[8] S. Catani, M. Ciafoloni and F. Hautmann, Nucl. Phys. B **366**, 135 (1991).

[9] J.C. Collins and R.K. Ellis, Nucl. Phys. B **360**, 3 (1991).

[10] L.V. Gribov, E.M. Levin, and M.G. Ryskin, Phys. Rep. **100**, 1 (1983).

[11] E.M. Levin, M.G. Ryskin, Yu.M. Shabelsky and A.G. Shuvaev, Sov. J. Nucl. Phys. **53**, 657 (1991).

[12] E.A. Kuraev, L.N. Lipatov, and V.S. Fadin, Sov. Phys. JETP **44**, 443 (1976);
E.A. Kuraev, L.N. Lipatov, and V.S. Fadin, Sov. Phys. JETP **45**, 199 (1977);
I.I. Balitsky and L.N. Lipatov, Sov. J. Nucl. Phys. **28**, 822 (1978).

[13] M. Ciafaloni, Nucl. Phys. B **296**, 49 (1988);
S. Catani, F. Fiorani, and G. Marchesini, Phys. Lett. B **234**, 339 (1990);
S. Catani, F. Fiorani, and G. Marchesini, Nucl. Phys. B **336**, 18 (1990);
G. Marchesini, Nucl. Phys. B **445**, 49 (1995).

[14] V.N. Gribov and L.N. Lipatov, Yad. Fiz. **15**, 781 (1972);
L.N. Lipatov, Sov. J. Nucl. Phys. **20**, 94 (1975);
G. Altarelly and G. Parizi, Nucl. Phys. B **126**, 298 (1977);
Y.L. Dokshitzer, Sov. Phys. JETP **46**, 641 (1977).

[15] M.G. Ryskin and Yu.M. Shabelsky, Z. Phys. C **61**, 517 (1994);
M.G. Ryskin, Yu.M. Shabelsky and A.G. Shuvaev, Z. Phys. C **69**, 269 (1996).

[16] S.P. Baranov and M. Smizanska, Phys. Rev. D **62**, 014012 (2000).

[17] Ph. Hägler, R. Kirschner, A. Schäfer, L. Szymanowski and O.V. Teryaev, Phys. Rev. D **62**, 071502 (2000).

[18] H. Jung, Phys. Rev. D **65**, 034015 (2002).

[19] A.V. Lipatov, N.P. Zotov, and V.A. Saleev, Yad. Fiz. **66**, 786 (2003);
S.P. Baranov, N.P. Zotov and A.V. Lipatov, Phys. Atom. Nucl. **67**, 834 (2004).

[20] A.V. Lipatov, L. Lönnblad, and N.P. Zotov, JHEP **01**, 010 (2004).

[21] H. Jung, Mod. Phys. Lett. A **19**, 1 (2004).

[22] L. Motyka and N. Timneanu, Eur. Phys. J. **C27**, 73 (2003).

[23] M. Hansson, H. Jung, and L. Jönsson, hep-ph/0402019.

[24] A.V. Lipatov and N.P. Zotov, Eur. Phys. J. C **41**, 163 (2005).

[25] A.V. Lipatov, to be published in Yad. Fiz. (2006).

[26] H. Jung and G. Salam, Eur. Phys. J. C **19**, 351 (2001).

[27] H. Jung, Comput. Phys. Comm. **143**, 100 (2002).

[28] S.P. Baranov and N.P. Zotov, Phys. Lett. B **491**, 111 (2000).

[29] S.P. Baranov, H. Jung, L. Jönsson, S. Padhi, and N.P. Zotov, Eur. Phys. J. C **24**, 425 (2002).

[30] A.V. Lipatov and N.P. Zotov, DESY 05-252 [hep-ph/0512013].

[31] J. Kwiecinski, A.D. Martin and A.M. Stasto, Phys. Rev. D **56**, 3991 (1997).

[32] M.A. Kimber, A.D. Martin and M.G. Ryskin, Phys. Rev. D **63**, 114027 (2001);
G. Watt, A.D. Martin and M.G. Ryskin, Eur. Phys. J. C **31**, 73 (2003).

[33] G.P. Lepage, J. Comput. Phys. **27**, 192 (1978).

[34] B. Andersson *et al.* (Small-x Collaboration), Eur. Phys. J. C **25**, 77 (2002).

[35] J. Andersen *et al.* (Small-x Collaboration), Eur. Phys. J. C **35**, 77 (2004).

[36] J. Kwiecinski, A.D. Martin and A. Sutton, Phys. Rev. D **52**, 1445 (1995).

[37] J. Kwiecinski, A.D. Martin and J. Outhwaite, Eur. Phys. J. C **9**, 611 (2001).

[38] A.V. Lipatov and N.P. Zotov, Eur. Phys. J. C **27**, 87 (2003).

[39] N.P. Zotov, I.I. Katkov, and A.V. Lipatov, to be published in Yad. Fiz (2006).

[40] M. Glück, E. Reya and A. Vogt, Phys. Rev. **D46**, 1973 (1992);
M. Glück, E. Reya and A. Vogt, Z. Phys. **C67**, 433 (1995).

[41] A.V. Lipatov and N.P. Zotov, Phys. Rev. D **72**, 054002 (2005).

[42] M.A. Kimber, A.D. Martin and M.G. Ryskin, Eur. Phys. J. C **12**, 655 (2001).

[43] A.V. Lipatov and N.P. Zotov, DESY 05-157 [hep-ph/0507243].

[44] S. Frixione, P. Nason, and G. Ridolfi, Nucl. Phys. B **454**, 3 (1995).

[45] C. Peterson, D. Schlatter, I. Schmitt, and P. Zerwas, Phys. Rev. D **27**, 105 (1983).

[46] T. Sjöstrand *et al.* Comput. Phys. Comm. **135**, 238 (2001).

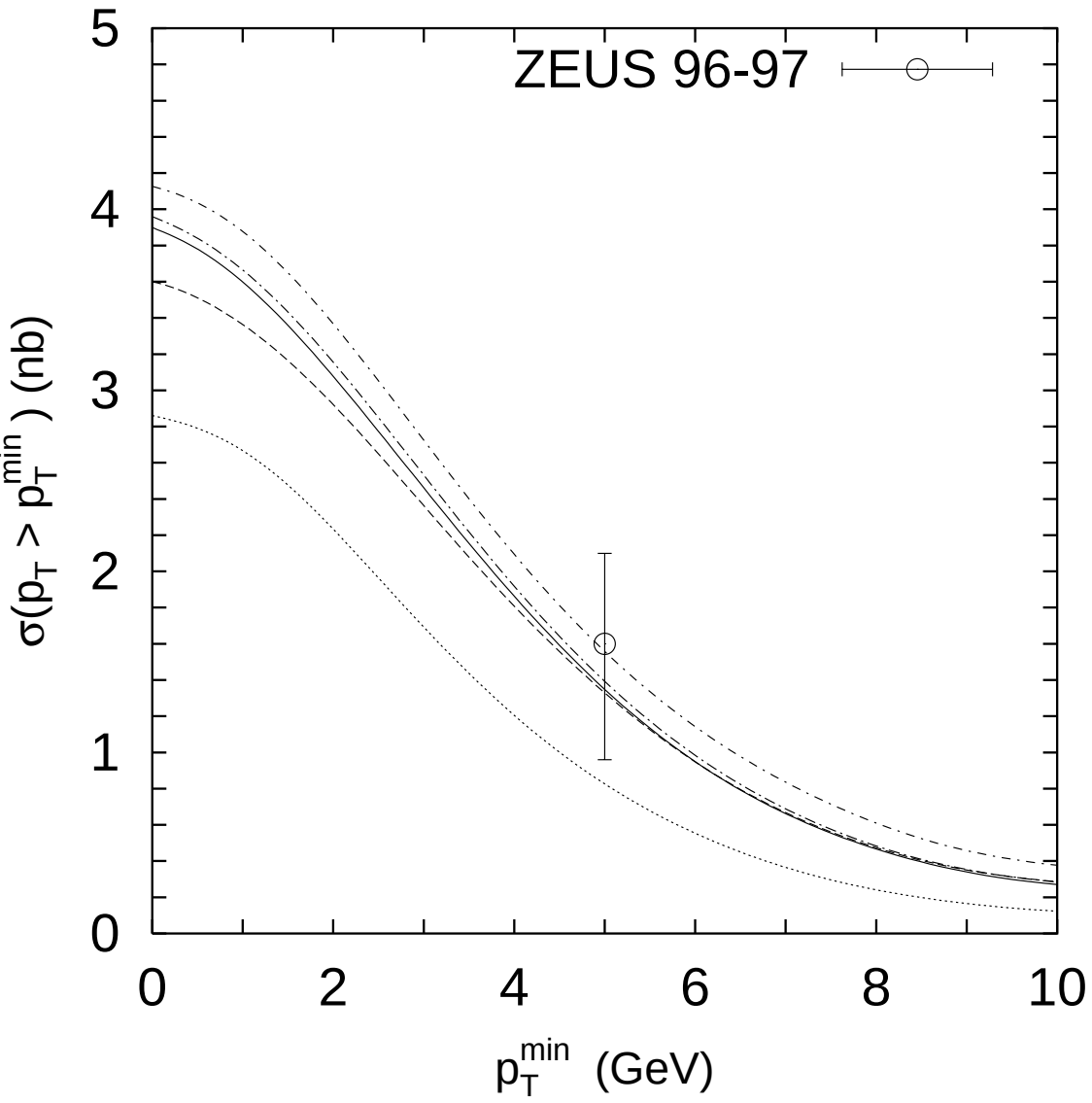

Figure 1: The inclusive beauty cross section as a function of $p_T^{\rm min}$ calculated at $|\eta^b| < 2$, $Q^2 < 1$ GeV^2 and $0.2 < y < 0.8$. The solid, dashed, dash-dotted, dotted and short dash-dotted curves correspond to the J2003 set 1 — 3, KMR and KMS unintegrated gluon distributions, respectively. The experimental data are from ZEUS [5].

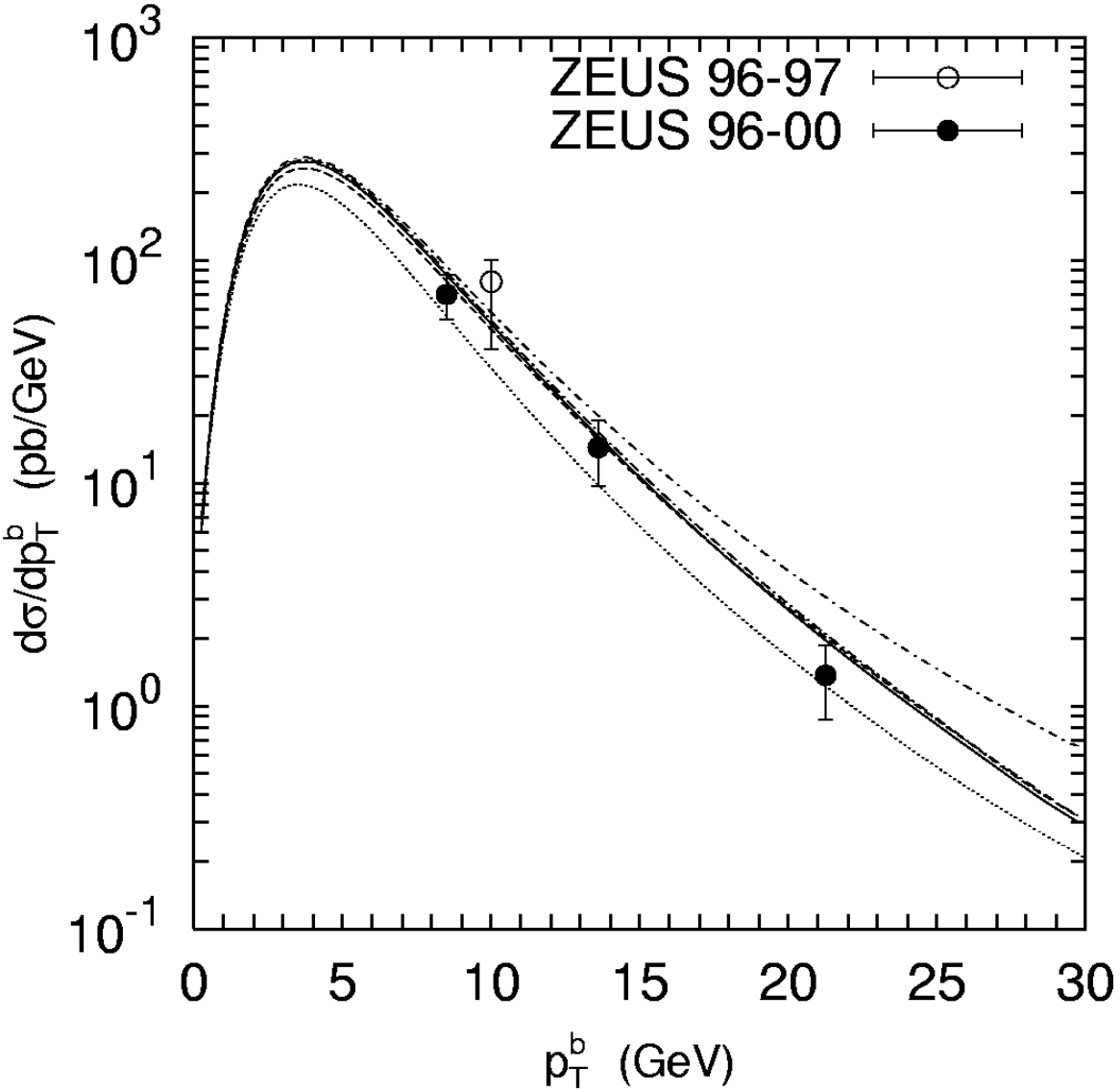

Figure 2: The differential cross section $d\sigma/dp_T^b$ for the inclusive beauty production calculated at $|\eta^b| < 2$, $Q^2 < 1$ GeV^2 and $0.2 < y < 0.8$. All curves are the same as in Fig. 1. The experimental data are from ZEUS [5, 6].

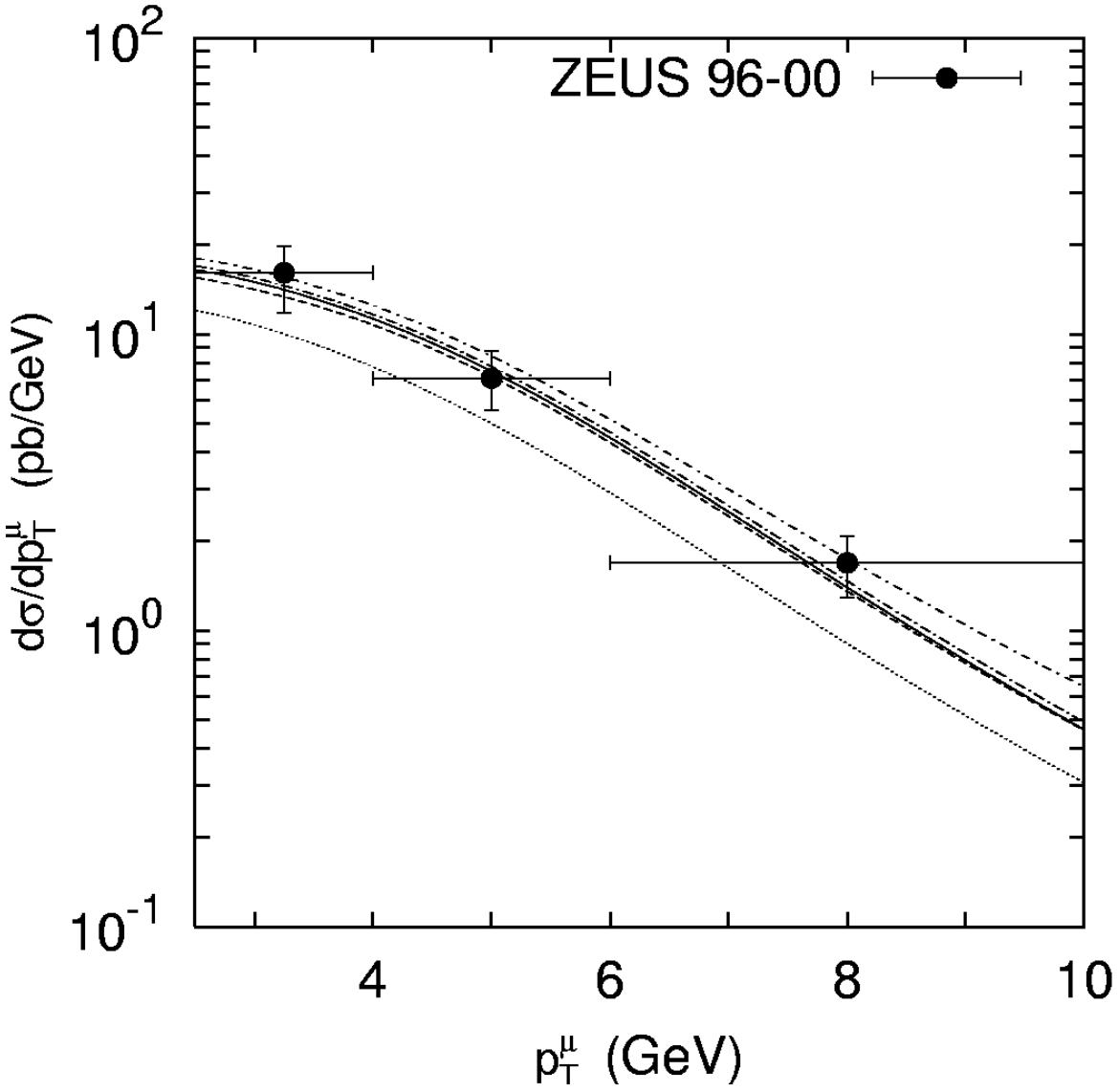

Figure 3: The differential cross section $d\sigma/dp_T^\mu$ for dijets with an associated muon coming from b decays in the kinematic range $-1.6 < \eta^\mu < 2.3$, $Q^2 < 1$ GeV^2, $0.2 < y < 0.8$, $p_T^{\mathrm{jet}_1} > 7$ GeV, $p_T^{\mathrm{jet}_2} > 6$ GeV and $|\eta^{\mathrm{jet}}| < 2.5$. All curves are the same as in Fig. 1. The experimental data are from ZEUS [6].

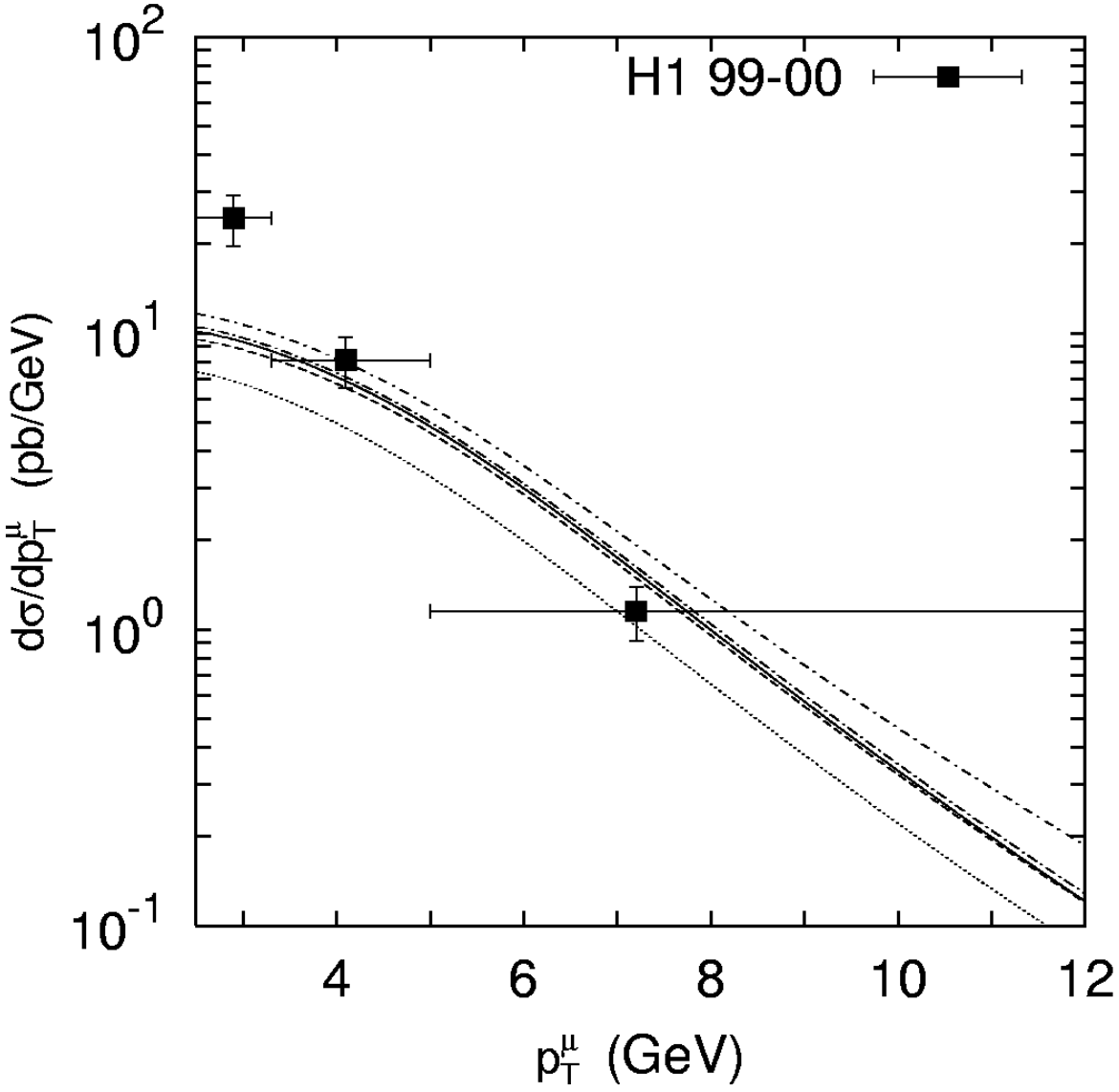

Figure 4: The differential cross section $d\sigma/dp_T^\mu$ for dijets with an associated muon coming from b decays in the kinematic range $-0.55 < \eta^\mu < 1.1$, $Q^2 < 1$ GeV^2, $0.2 < y < 0.8$, $p_T^{\mathrm{jet}_1} > 7$ GeV, $p_T^{\mathrm{jet}_2} > 6$ GeV and $|\eta^{\mathrm{jet}}| < 2.5$. All curves are the same as in Fig. 1. The experimental data are from H1 [7].

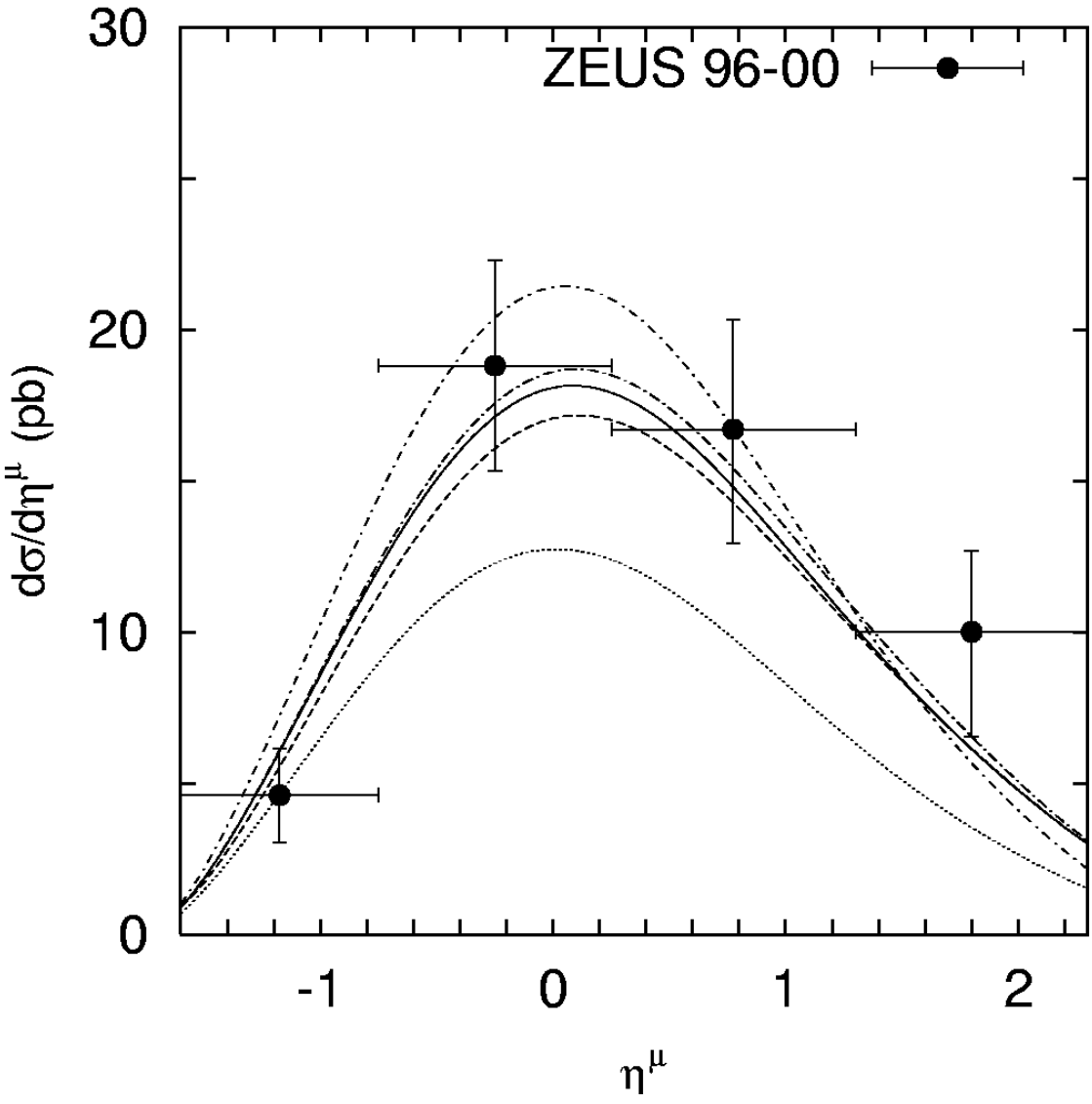

Figure 5: The differential cross section $d\sigma/d\eta^{\mu}$ for dijets with an associated muon coming from b decays in the kinematic range $p_T^{\mu} > 2.5$ GeV, $Q^2 < 1$ GeV^2, $0.2 < y < 0.8$, $p_T^{\mathrm{jet}_1} > 7$ GeV, $p_T^{\mathrm{jet}_2} > 6$ GeV and $|\eta^{\mathrm{jet}}| < 2.5$. All curves are the same as in Fig. 1. The experimental data are from ZEUS [6].

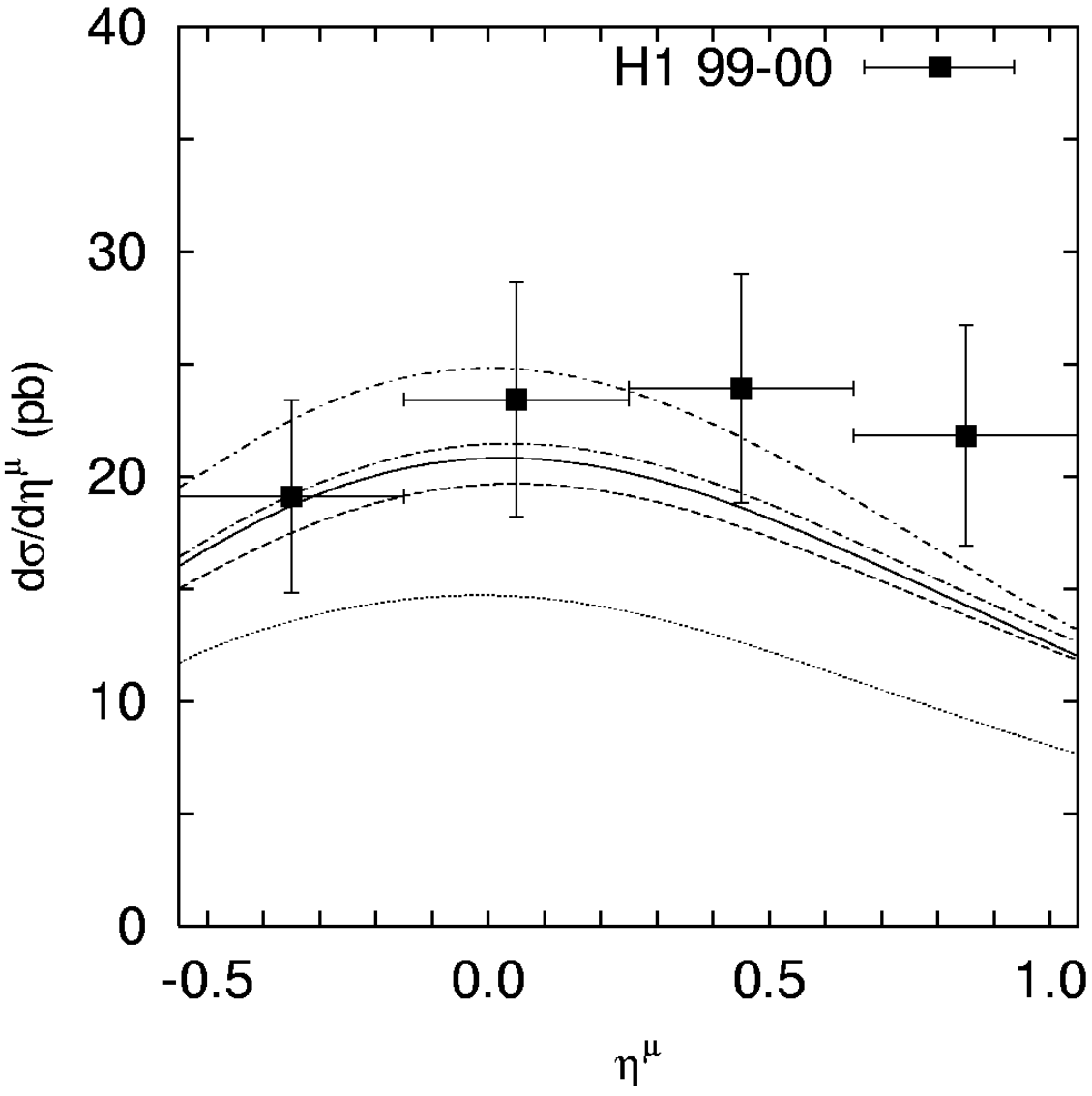

Figure 6: The differential cross section $d\sigma/d\eta^{\mu}$ for dijets with an associated muon coming from b decays in the kinematic range $p_T^{\mu} > 2.5$ GeV, $Q^2 < 1$ GeV^2, $0.2 < y < 0.8$, $p_T^{\mathrm{jet}_1} > 7$ GeV, $p_T^{\mathrm{jet}_2} > 6$ GeV and $|\eta^{\mathrm{jet}}| < 2.5$. All curves are the same as in Fig. 1. The experimental data are from H1 [7].

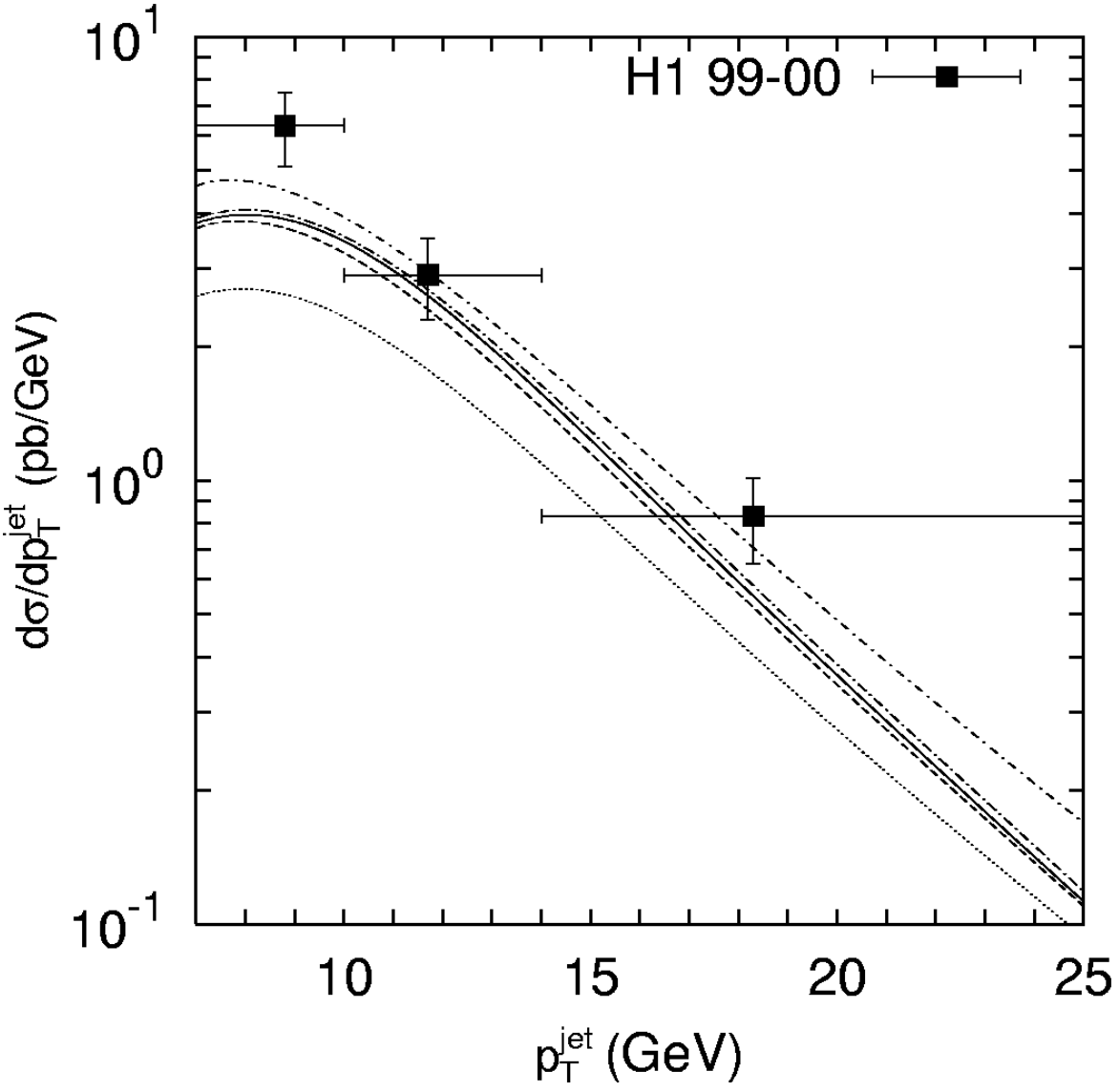

Figure 7: The leading jet transverse momentum distribution $d\sigma/dp_T^{\rm jet}$ for dijets with an associated muon coming from b decays in the kinematic range $-0.55 < \eta^\mu < 1.1$, $Q^2 < 1$ GeV^2, $0.2 < y < 0.8$, $p_T^{\rm jet_1} > 7$ GeV, $p_T^{\rm jet_2} > 6$ GeV and $|\eta^{\rm jet}| < 2.5$. All curves here are the same as in Fig. 1. The experimental data are from H1 [7].

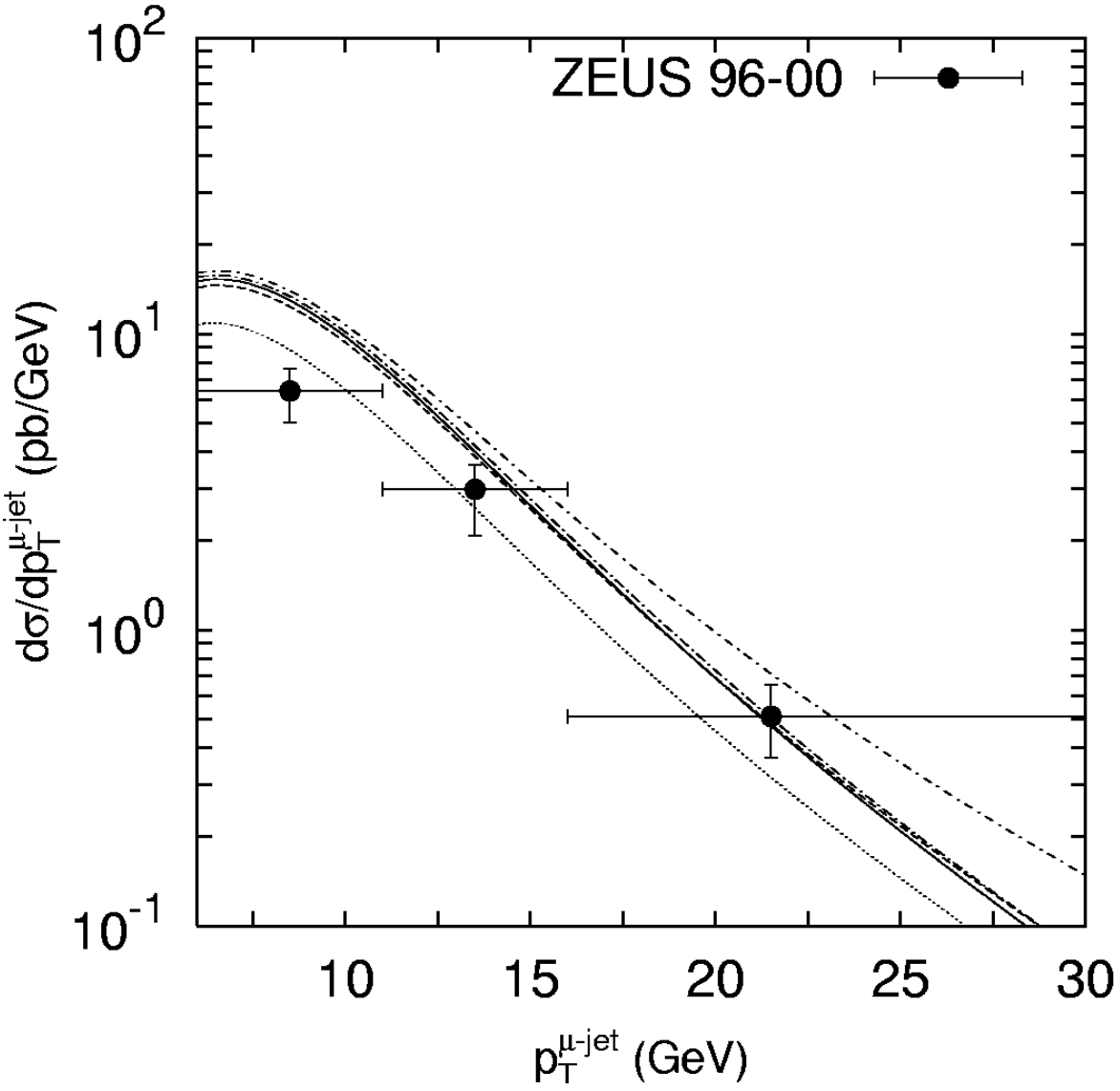

Figure 8: The transverse momentum distribution of the jet associated to the muon coming from b decays in the kinematic range $-0.55 < \eta^{\mu} < 1.1$, $p_T^{\mu} > 2.5$ GeV, $Q^2 < 1$ GeV^2, $0.2 < y < 0.8$ and $|\eta^{\mu-\text{jet}}| < 2.5$. All curves are the same as in Fig. 1. The experimental data are from ZEUS [6].

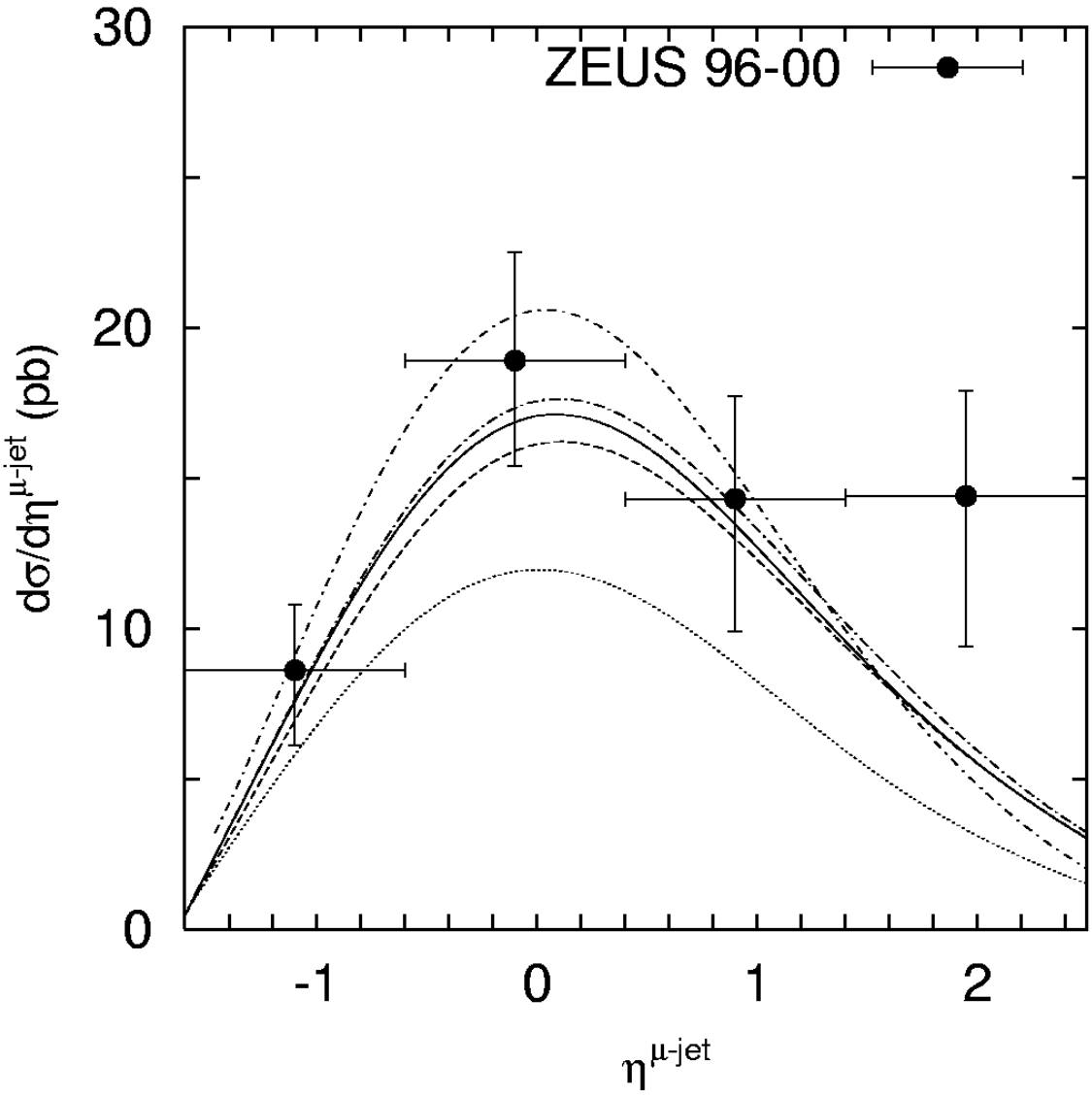

Figure 9: The pseudo-rapidity distribution of the jet associated to the muon coming from b decays in the kinematic range $-0.55 < \eta^{\mu} < 1.1$, $p_T^{\mu} > 2.5$ GeV, $Q^2 < 1$ GeV^2, $0.2 < y < 0.8$ and $p_T^{\mu-\mathrm{jet}} > 6$ GeV. All curves are the same as in Fig. 1. The experimental data are from ZEUS [6].

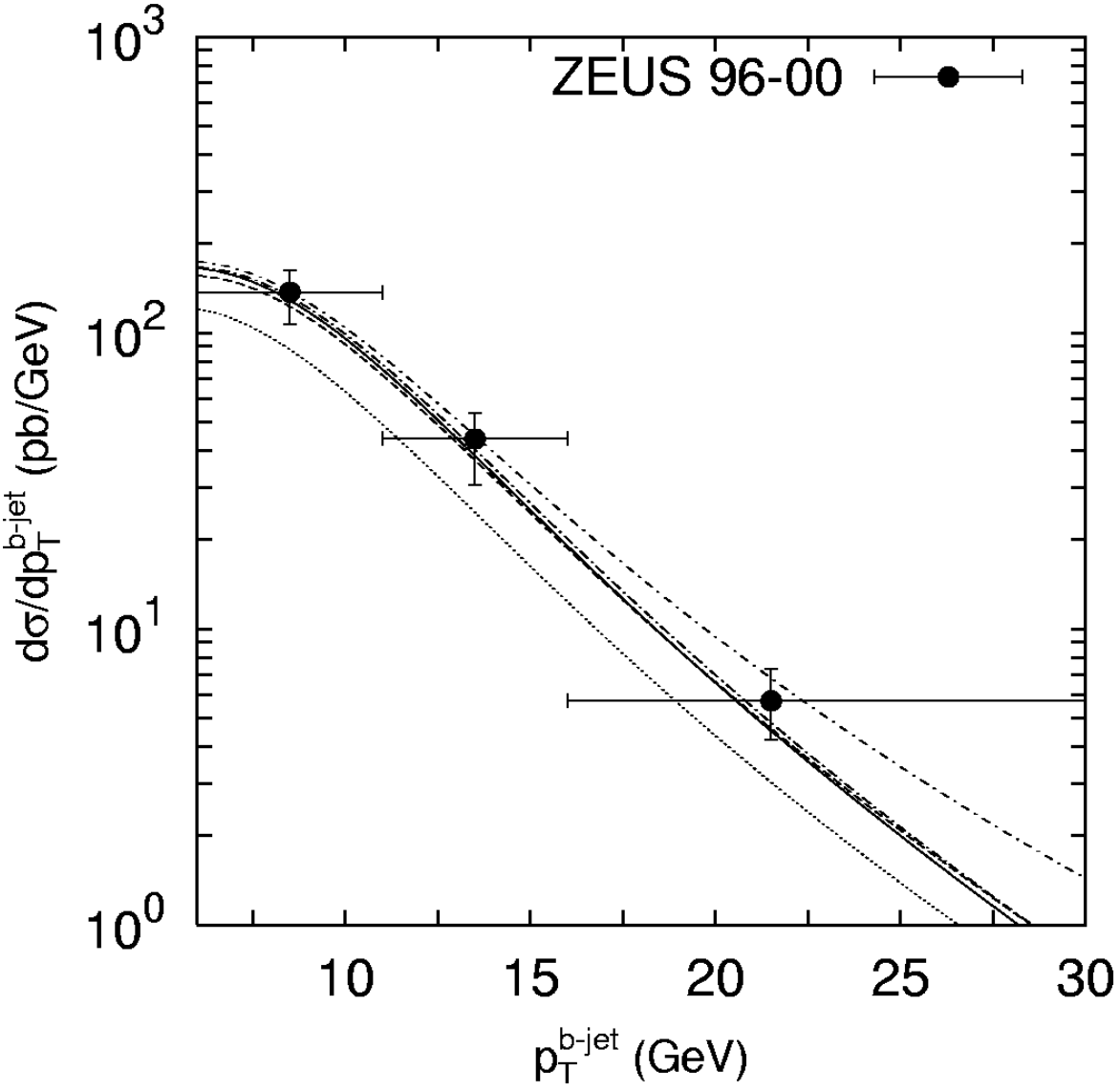

Figure 10: The transverse momentum distribution of the jet containing a B-hadron in the kinematic range $-0.55 < \eta^{\mu} < 1.1$, $p_T^{\mu} > 2.5$ GeV, $Q^2 < 1$ GeV^2, $0.2 < y < 0.8$ and $|\eta^{b-\mathrm{jet}}| < 2.5$. All curves are the same as in Fig. 1. The experimental data are from ZEUS [6].

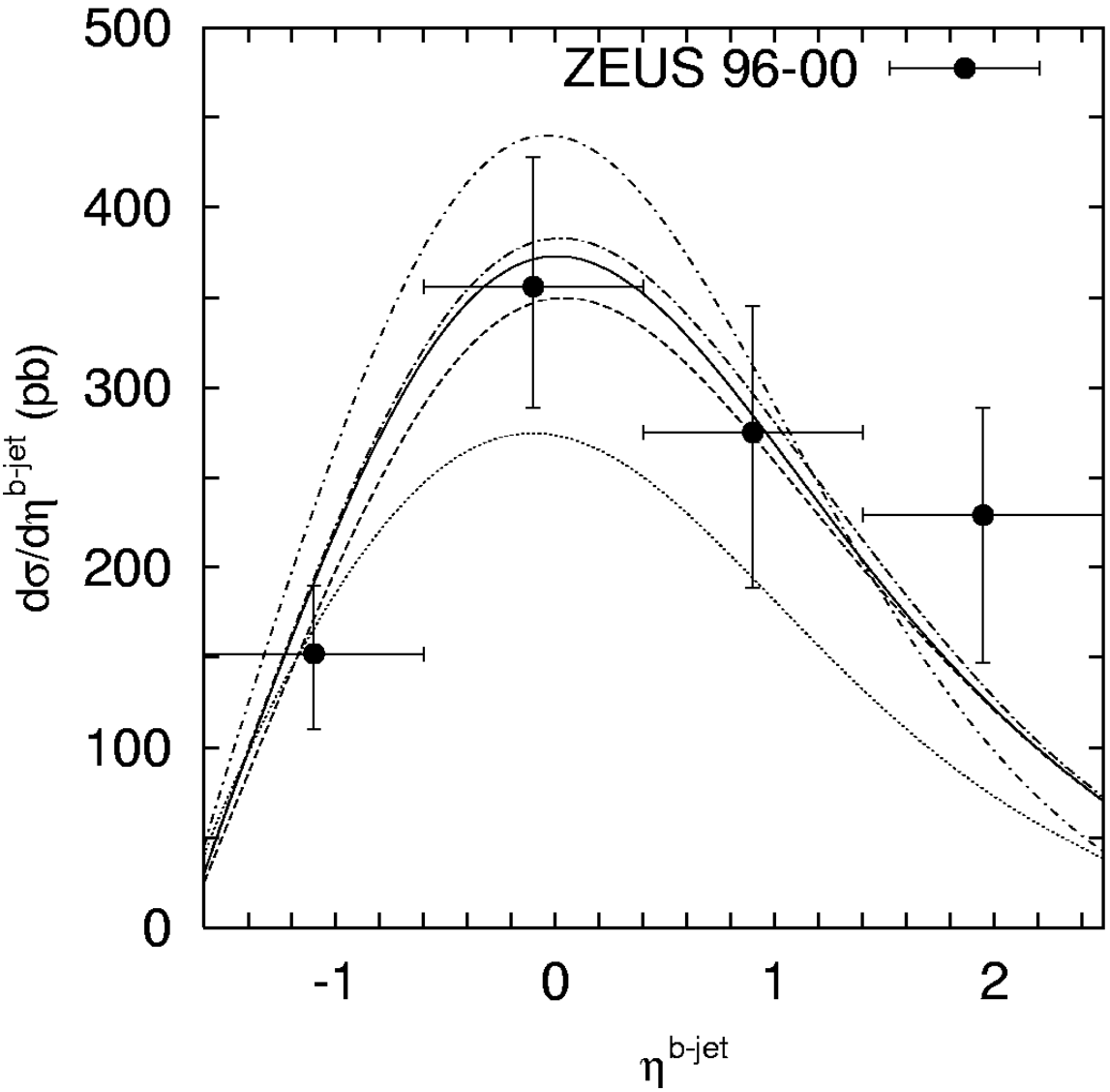

Figure 11: The pseudo-rapidity distribution of the jet containing a B-hadron in the kinematic range $-0.55 < \eta^{\mu} < 1.1$, $p_T^{\mu} > 2.5$ GeV, $Q^2 < 1$ GeV^2, $0.2 < y < 0.8$ and $|\eta^{b-\mathrm{jet}}| < 2.5$. All curves are the same as in Fig. 1. The experimental data are from ZEUS [6].

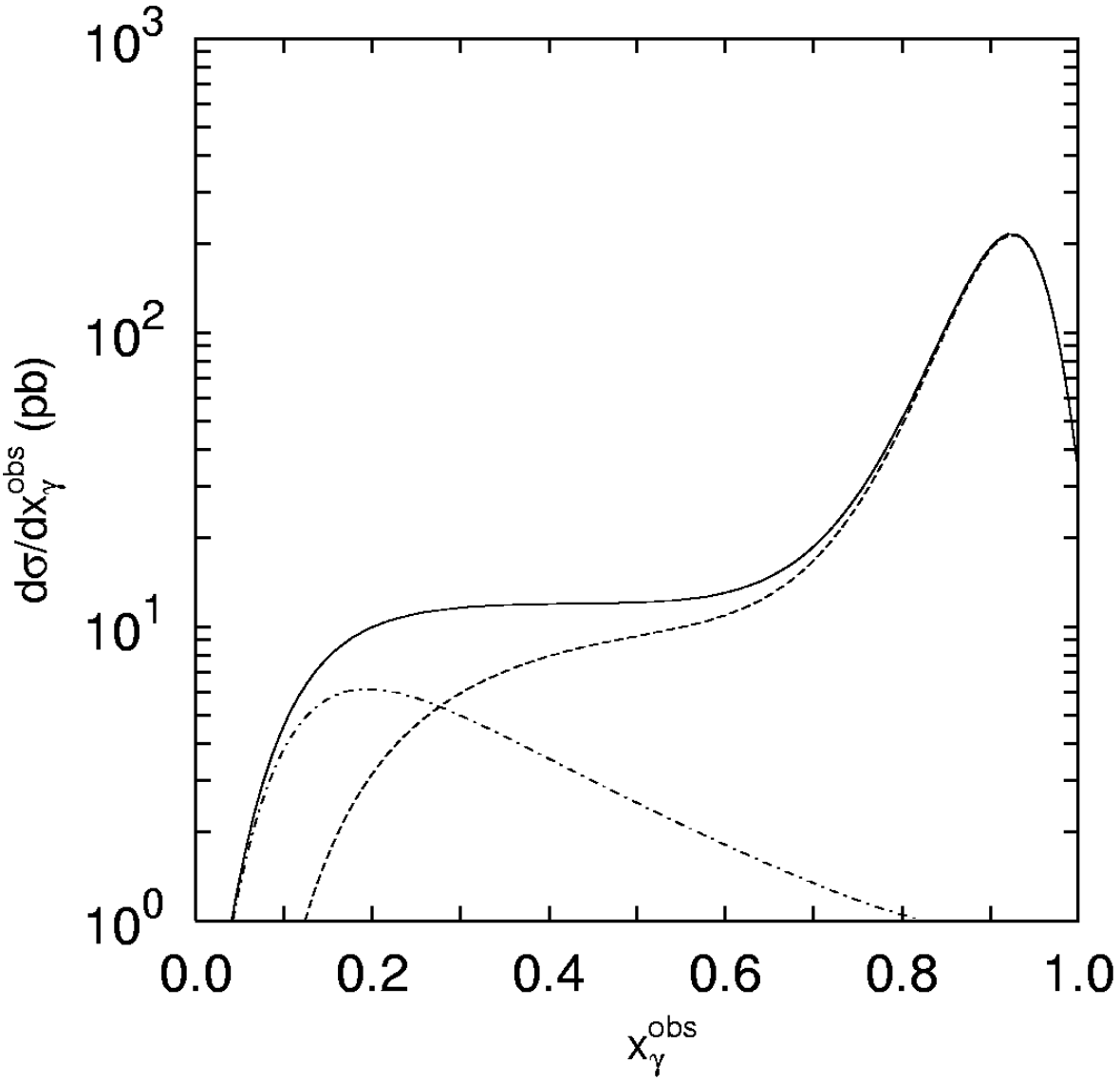

Figure 12: The differential cross section $d\sigma/dx_\gamma^{\rm obs}$ for dijets with an associated muon coming from b decays in the kinematic range $-1.6 < \eta^\mu < 2.3$, $p_T^\mu > 2.5$ GeV, $Q^2 < 1$ GeV^2, $0.2 < y < 0.8$, $p_T^{\rm jet_1} > 7$ GeV, $p_T^{\rm jet_2} > 6$ GeV and $|\eta^{\rm jet}| < 2.5$. Separately shown the contributions from the photon-gluon (dashed curve) and gluon-gluon fusion (dash-dotted curve). Solid curve represents the sum of both these contributions. The KMR unintegrated gluon densities in a proton and in a photon has been used.

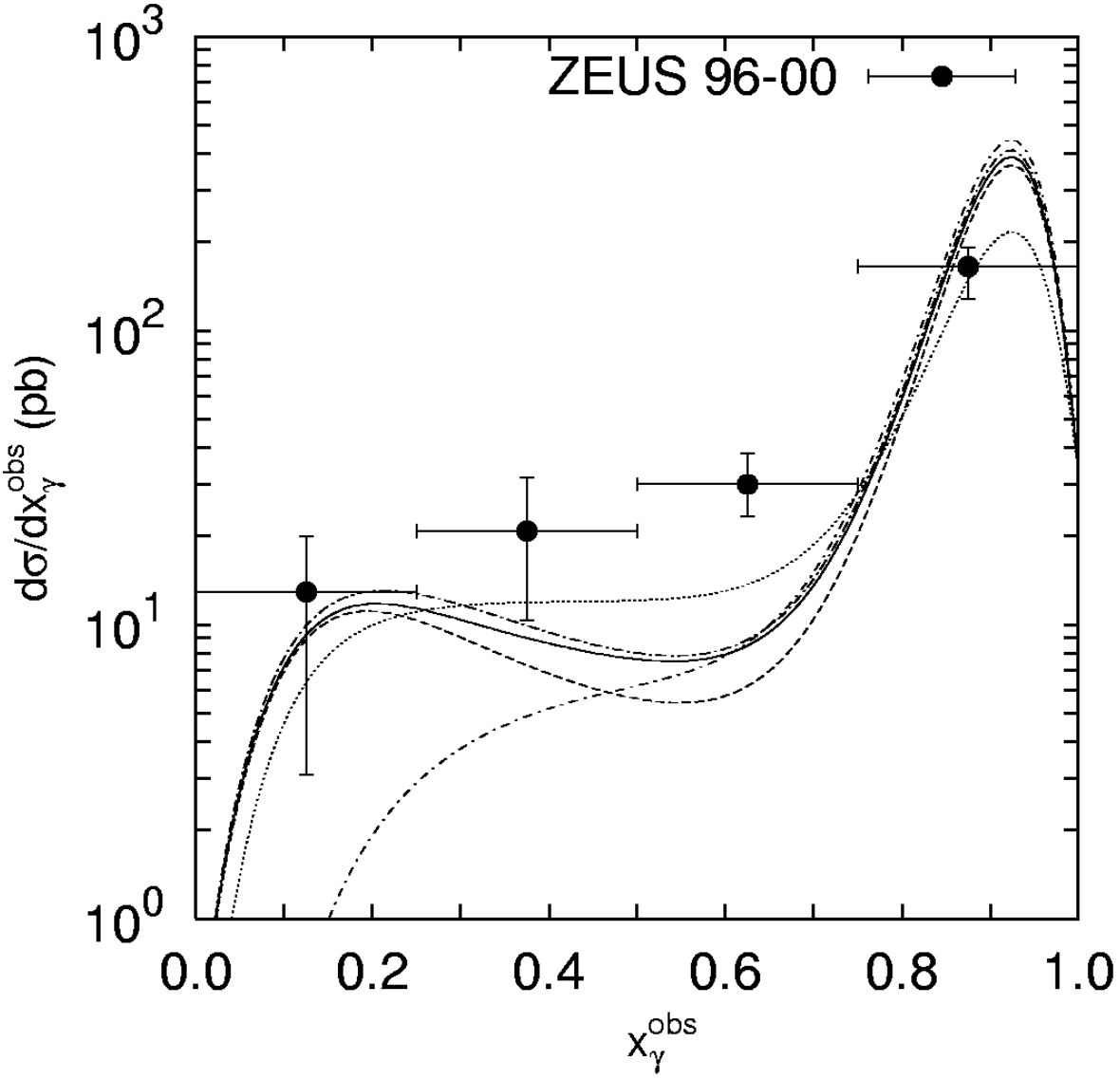

Figure 13: The differential cross section $d\sigma/dx_\gamma^{\rm obs}$ for dijets with an associated muon coming from b decays in the kinematic range $-1.6 < \eta^\mu < 2.3$, $p_T^\mu > 2.5$ GeV, $Q^2 < 1$ GeV^2, $0.2 < y < 0.8$, $p_T^{\rm jet_1} > 7$ GeV, $p_T^{\rm jet_2} > 6$ GeV and $|\eta^{\rm jet}| < 2.5$. All curves are the same as in Fig. 1. The experimental data are from ZEUS [6].

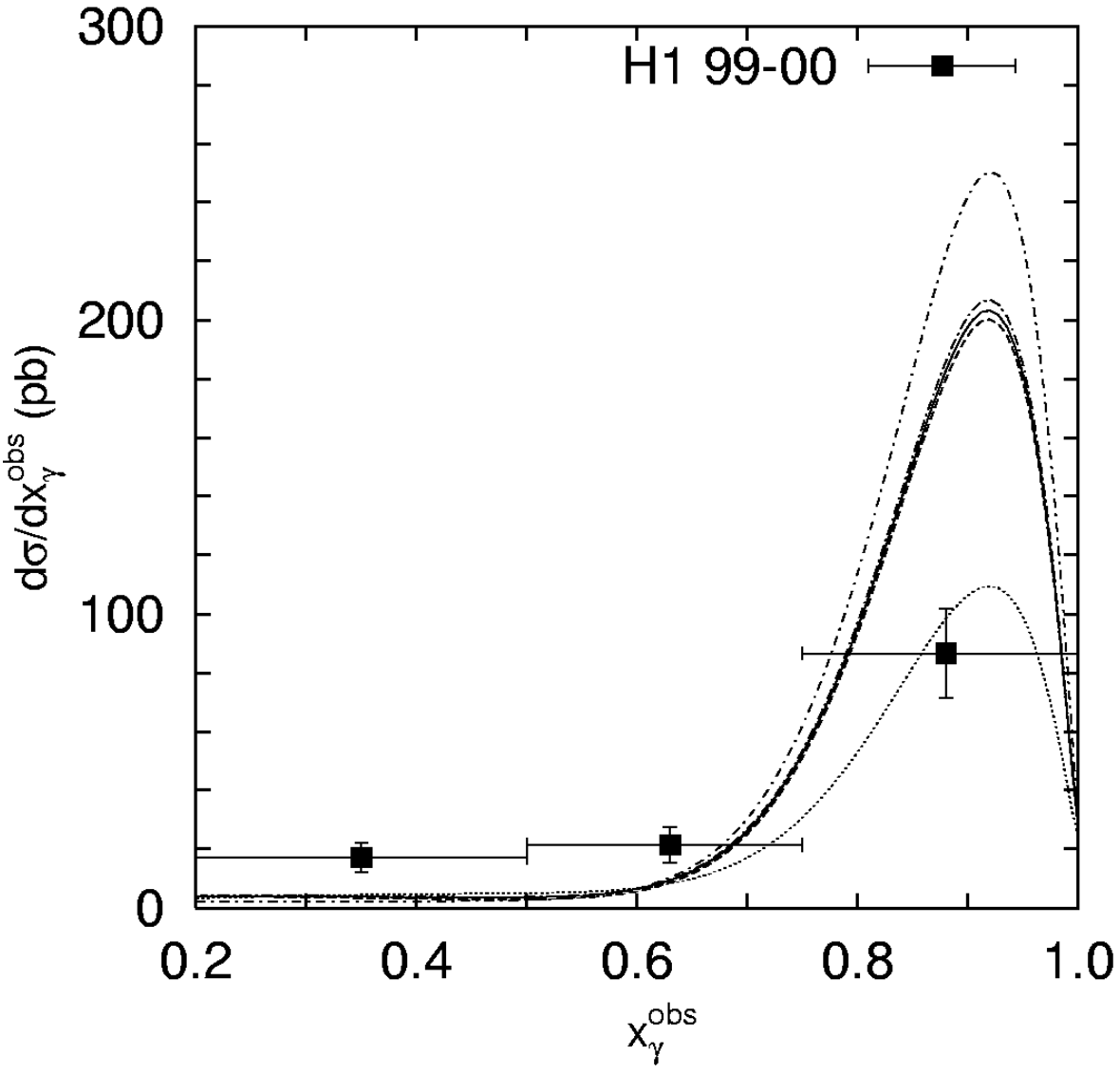

Figure 14: The differential cross section $d\sigma/dx_\gamma^{\rm obs}$ for dijets with an associated muon coming from b decays in the kinematic range $-0.55 < \eta^\mu < 1.1$, $p_T^\mu > 2.5$ GeV, $Q^2 < 1$ GeV^2, $0.2 < y < 0.8$, $p_T^{\rm jet_1} > 7$ GeV, $p_T^{\rm jet_2} > 6$ GeV and $|\eta^{\rm jet}| < 2.5$. All curves are the same as in Fig. 1. The experimental data are from H1 [7].

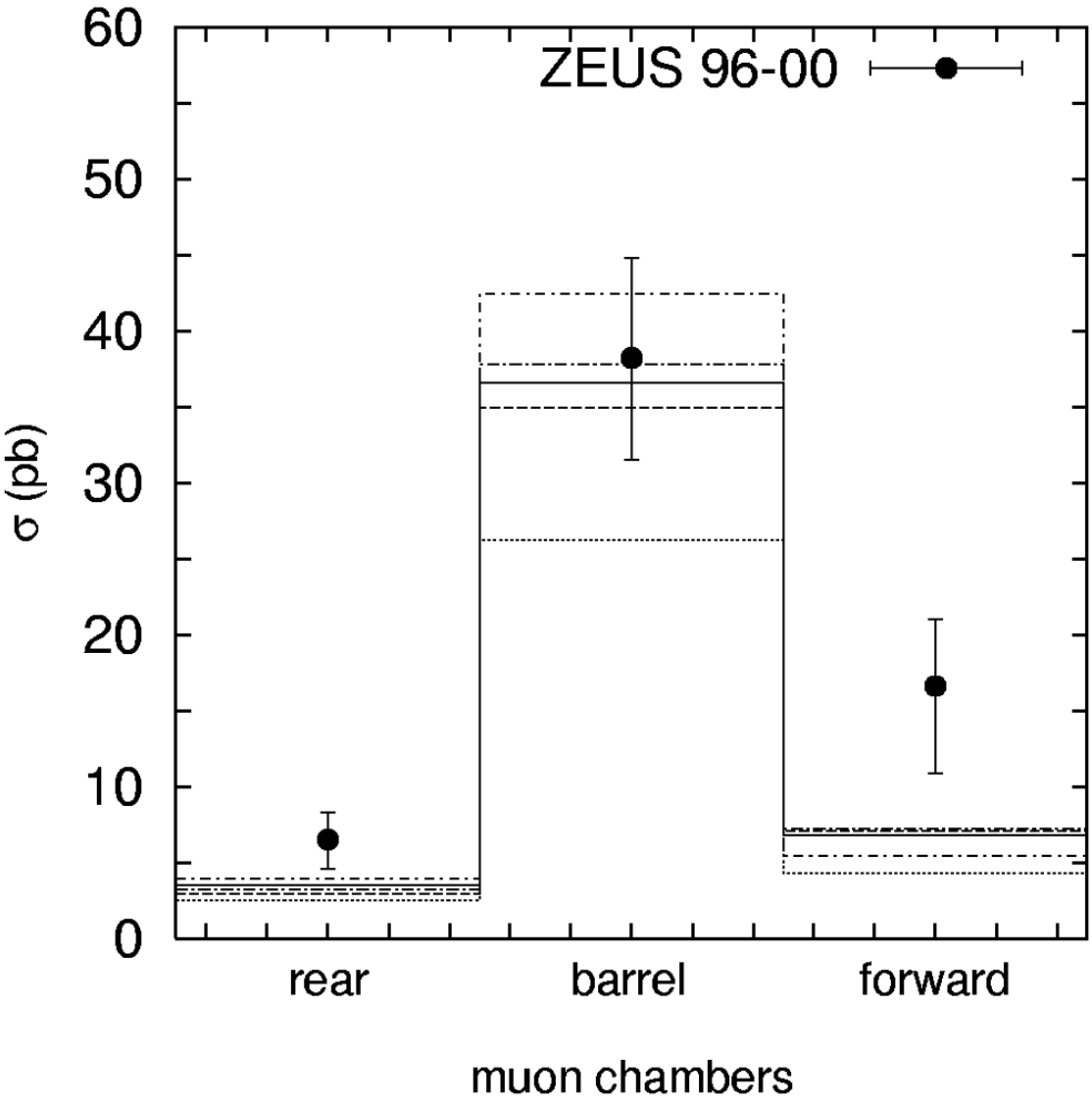

Figure 15: The cross section for muon coming from b decays in dijet events calculated in the rear, barrel and forward kinematical regions (see text). The cuts are applied: $Q^2 < 1$ GeV^2, $0.2 < y < 0.8$, $p_T^{\mathrm{jet}_1} > 7$ GeV, $p_T^{\mathrm{jet}_2} > 6$ GeV and $|\eta^{\mathrm{jet}}| < 2.5$. All curves are the same as in Fig. 1. The experimental data are from ZEUS [6].